NATIONAL ADVISORY COMMITTEE FOR AERQNAUTICS

TECHNICAL NOTE 3407

INTERACTION OF A FREE FLAME FRONT

WITH A TURBULENCE FIELD

By Maurice Tucker

Lewis Flight Propulsion Laboratory
Cleveland, Ohio

NACA

Washington
March 1955

TABLE OF CONTENTS

3493

NATIONAL ADVISORY COMMITTEE FOR AERONAUTICS

TECHNICAL NOTE 3407

INTERACTION OF A FREE FLAME FRONT WITH A TURBULENCE FIELD

By Maurice Tucker

SUMMARY

Small-perturbation spectral-analysis techniques are used to obtain the root-mean-square flame-generated turbulence velocities and the attenuating pressure fluctuations stemming from interaction of a constant-pressure flame front with a field of isotropic turbulence in the absence of turbulence-decay processes.

The anisotropic flame-generated turbulence velocities are found to be of about the same intensity as those of the incident isotropic turbulence, the lateral turbulence velocities being always lower but the longitudinal velocity is somewhat increased for flame-temperature ratios in excess of 7. The small-perturbation analysis indicates that the incremental turbulent flame speed is a second-order quantity composed of two parts: One part represents the root-mean-square area of the turbulent flame front; the other represents the contribution of the transverse velocity fluctuations which results from the flame-front distortion. Directly at the flame front the noise-pressure levels of the pressure fluctuations are fairly intense (59 to 81 decibels referred to 0.0002 dyne/sq cm) even at moderate approach-flow turbulence intensities.

INTRODUCTION

Development of high-output jet engines has stimulated interest in the role played by turbulence in combustion phenomena. In the earliest studies of flame-turbulence interaction, Damkohler (ref. 1) and Shelkin (ref. 2) utilized mixing-length theories of turbulence to obtain semi-quantitative relations for predicting flame speeds. Damkohler introduced the concept that turbulence of a scale large relative to the flame-front thickness increases the average flame speed by increasing the instantaneous flame surface area. The authors of reference 3 were unable to confirm the relations of references 1 or 2 by their experimental values of turbulent flame speed in Bunsen burners. Experiments on flames stabilized in channels (ref. 4) suggested that approach-flow turbulence had little effect on burning velocity and that the disturbances affecting turbulent flame speed were primarily flame-generated. A similar conclusion was arrived at in reference 5.

In an attempt to obtain agreement between theory and experiment, Karlovitz, Denniston, and Wells (ref. 6) and Scurlock and Grover (ref. 7) have incorporated the concept of flame-generated disturbances in their recent theories of turbulent flame speed which utilize G. I. Taylor's one-dimensional theory of diffusion by continuous movements. The somewhat arbitrary assumption is made in the analyses of both references 6 and 7 that these flame-generated disturbances constitute additional turbulence only. In reference 6 the energy of the flame-generated turbulence is taken as the difference between kinetic energy of the burned gas in the absence of turbulence and the kinetic energy obtained by using the average velocity of the burned gas normal to the turbulent flame front. In reference 7 the flame-generated turbulence energy is obtained from a momentum balance of unburned and burned gases before and after an assumed mixing of the burned gas.

The data obtained in reference 8 on pentane-air flames baffle-stabilized in a rectangular duct suggest that the methods of references 6 and 7 overestimate considerably the turbulence generated by flame - turbulence interaction. Apart from the question of validity of such methods of calculating flame-generated turbulence, objections have been raised (ref. 9) to calculations of flame speed made on the basis of a hypothetical upstream turbulence compounded from approach-stream turbulence and turbulence generated downstream of the flame as was done in reference 7 and implied in reference 6.

The present analysis is primarily concerned with the turbulence velocities and other fluctuation quantities associated with the linearized interaction of a free flame (not influenced by bounding walls) with turbulence present in the combustible mixture. Such turbulence will be referred to as approach-flow turbulence. The flame is treated as a discontinuity specified by the appropriate fundamental (laminar) flame speed and flame temperature. The interaction of such a flame front with a transverse plane wave, that is, a vorticity wave or shear wave, of arbitrary inclination relative to the front is first analyzed. The effects of an entire spectrum of transverse plane waves constituting a weak field of turbulence are then developed from the single-wave results. The statistical or root-mean-square fluctuation quantities describing the pressure fields and the anisotropic flame-generated turbulence resulting from interaction of the flame front with isotropic approach-flow turbulence are obtained for the limiting case of constant-pressure combustion. Some discussions of turbulent flame speed and of combustion noise are also presented.

FLAME - TURBULENCE INTERACTION PROCESS

Turbulent motion may be regarded as a Fourier superposition of a very large number of different-sized and randomly oriented component plane-wave motions. The customary assumptions concerning the turbulence

(see ref. 10) are also made in the present analysis - namely, that turbulent decay effects are negligible and that the density fluctuations
associated with the turbulence are also small enough to be neglected.
The first assumption, which implies inviscid flow and very small turbulent velocity fluctuations, permits linear superposition of the component waves. With the second assumption, the continuity equation requires that these Fourier waves be transverse plane waves, that is,
vorticity or shear waves. For each of these waves the local velocity
vector $\underline{A}$ is perpendicular to the vector $\underline{k}$, normal to the wave front.
The vector $\underline{k}$ is termed the wave-number vector; its magnitude k is
termed the wave number, which is defined as 2π divided by the wave
length. All symbols are defined in appendix A. Any one of the parallel
planes containing both the local velocity vector $\underline{A}$ and the wave-number
vector $\underline{k}$ is called the "polarization plane."

Because of the assumed linear superposition of the component waves,
the complete interaction results can be obtained from study of the interaction of a plane flame front with a single-component transverse wave
of the turbulence field. For simplicity this typical vorticity wave
will first be taken as a two-dimensional wave. Generalization to the
three-dimensional case will be made later. The configuration considered
is shown in sketch (a):

(a)
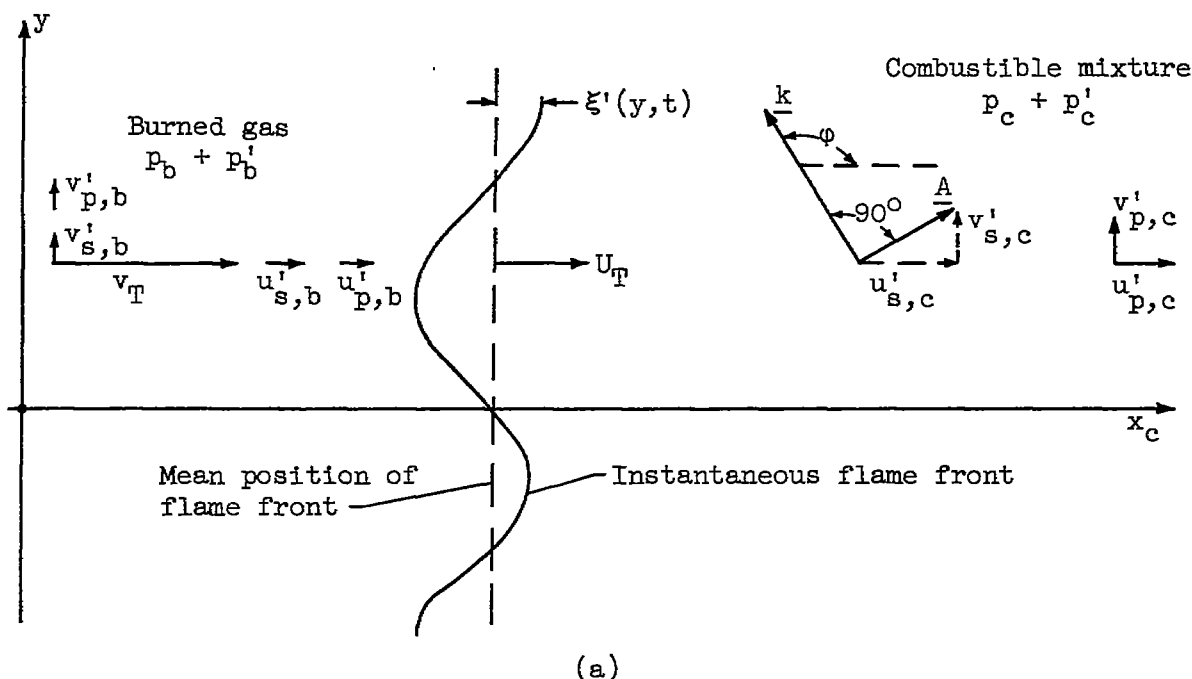
A flame front moves with mean velocity U_T into an inviscid combustible mixture. This mixture is at rest, but contains a vorticity wave with velocity vector $\underline{A}$ (components $u'_{s,c}$ and $v'_{s,c}$) and with wave-number vector $\underline{k}$ inclined at an angle φ to the positive direction of the x_c-axis. In the absence of any perturbation interaction, the plane front propagates into the combustible mixture with velocity U (the laminar flame speed). As indicated in appendix B, the motion of the burned gas whose velocity V is constant is away from the flame front. The flame front is assumed to be of infinite extent in directions transverse to the direction of the x_c-axis.

References 11 and 12 have shown that a weak inviscid disturbance field may be resolved into a stationary component and a moving component, both relative to the mean local flow. The moving component is an irrotational isentropic pressure-velocity disturbance. The stationary component, which is convected by the mean local flow, is a constant-pressure disturbance containing any vorticity fluctuations and entropy fluctuations present in the disturbance field. Thus, the interaction of the flame front with the vorticity wave would be expected to generate both an irrotational disturbance with velocity components $u'_{p,b}$, $v'_{p,b}$ and a rotational disturbance with velocity components $u'_{s,b}$, $v'_{s,b}$ in the burned gas, and an irrotational disturbance with velocity components $u'_{p,c}$, $v'_{p,c}$ in the combustible mixture. The resulting velocity fluctuations, which include both the irrotational and rotational disturbances, are designated as u'_c, v'_c and u'_b, v'_b for the combustible mixture and the burned gas, respectively. The flame front is displaced by an amount $\xi'(y,t)$ from its mean or unperturbed position as a result of the interaction.

The diagrams of figure 1, which are similar to those used in reference 12, may prove helpful in visualizing the interaction process. Suppose that at some instant t_1 the flame intersects a front of the vorticity wave at point P_1 of figure 1(a). At a later time $t_1 + \delta t$, the flame has moved a distance $U\delta t$ and now intersects the stationary vorticity wave front at point P_2. A vorticity wave with front parallel to line QP_2 is then produced in the burned gas. A cylindrical sound wave is generated at point P_1 at time t_1 and propagates at speed a_b into the burned gas while being convected with velocity $-V$. Another cylindrical wave is generated at point P_1 at time t_1 and propagates into the combustible mixture with speed a_c. The cylindrical wave fronts thus generated form envelopes (Mach lines) in both the combustible mixture and the burned gas which constitute plane sound waves.

For the wave-inclination angle φ shown in figure 1(b), an envelope cannot be formed on the burned-gas side of the flame front. The

3493

cylindrical sound waves thus expand independently and are thereby atten-
uated. On the combustible-mixture side of the front, the cylindrical
sound waves meet at the common tangent point P_2. For inclination an-
gles less than the critical angle shown, attenuating pressure waves are
also produced in the combustible mixture until another critical angle
$180° - \varphi$ is reached. Below this second critical angle, plane sound
waves are again obtained. These critical angles may be obtained from
the geometry of figure 1(b). For small flame Mach numbers where $M \equiv \dfrac{U}{a_c}$,

$$\varphi_{cr,c} = \sin^{-1} M$$

$$\varphi_{cr,b} = \sin^{-1} \left(\frac{M}{\sqrt{\tau}} \right)$$

As the flame Mach number M decreases, attenuating waves are produced
for a wider range of inclination angle. In the limiting case of very
slow flow (constant-pressure combustion),[1] only attenuating pressure
waves appear in combination with the vorticity waves if $0° < \varphi < 180°$.
Quantities associated with the pressure wave vanish when $\varphi = 0°$ or
$180°$ because the incident vorticity wave then passes through the com-
bustion front without distorting the front.

SINGLE-WAVE ANALYSIS

Two-Dimensional Formulation

    The interaction process described in the preceding section is now
formulated analytically for the passage of a combustion front through
a single weak two-dimensional vorticity wave of constant density in-
clined to the flame front. The case of a vorticity wave in three di-
mensions is considered later.

    The combustion front is assumed to be completely specified by its
laminar flame velocity U and the ratio of stagnation temperatures τ
in the burned gas and in the combustible mixture, respectively. In
the absence of any perturbations, the equations for conservation of
momentum, energy, and mass-flow rate, respectively, as written for a
reference frame moving with the flame front, are

---

[1]It can be shown that the static-pressure ratio across a flame
front is given by $p_b/p_c = 1 - \gamma(\tau - 1)M^2 + \cdots$

$$\left. \begin{aligned}
p_c + \rho_c U^2 &= p_b + \rho_b (U - V)^2 \\
\tau \left(\frac{\gamma R_g}{\gamma - 1} T_c + \frac{1}{2} U^2 \right) &= \frac{\gamma R_g}{\gamma - 1} T_b + \frac{1}{2} (U - V)^2 \\
\rho_c U &= \rho_b (U - V)
\end{aligned} \right\} \tag{1}$$

where subscripts c and b designate stations in the combustible mixture and in the burned gas, respectively. For simplicity it has been assumed that the combustion process does not entail a change in the number of moles per unit mass of gas; also, differences in the ratio of specific heats for the burned and unburned gas are ignored. The quantity $(\tau - 1)$ is then indicative of the increase in stagnation enthalpy or heat release.

For the interaction problem the resulting flame-front distortion $\xi'(y,t)$ must be considered in addition to the generated disturbances previously mentioned. Thus, both the flame-front perturbation velocity $\frac{\partial \xi'}{\partial t} \equiv \xi_t'$ and the instantaneous flame-front slope $\frac{\partial \xi'}{\partial y} \equiv \xi_y'$ will appear in the equations of motion. The conservation equations may still be applied in a coordinate system moving instantaneously with the distorted flame front since extreme gradients occur across the front and small disturbances are postulated. The various perturbation quantities (designated by primes) are assumed to have zero space or time averages. The flame speed U_T (see sketch (b)) will thus include any time-independent contributions arising from the perturbations.

$-\xi'(y,t)$

$\beta \equiv \tan^{-1}(-\xi_y')$

v_b'

$-(U_T + \xi_t' - u_c')$

$-(U_T - V_T + \xi_t' - u_b')$

v_c'

$-(U + \delta U)$

Perturbed flame front

(b)
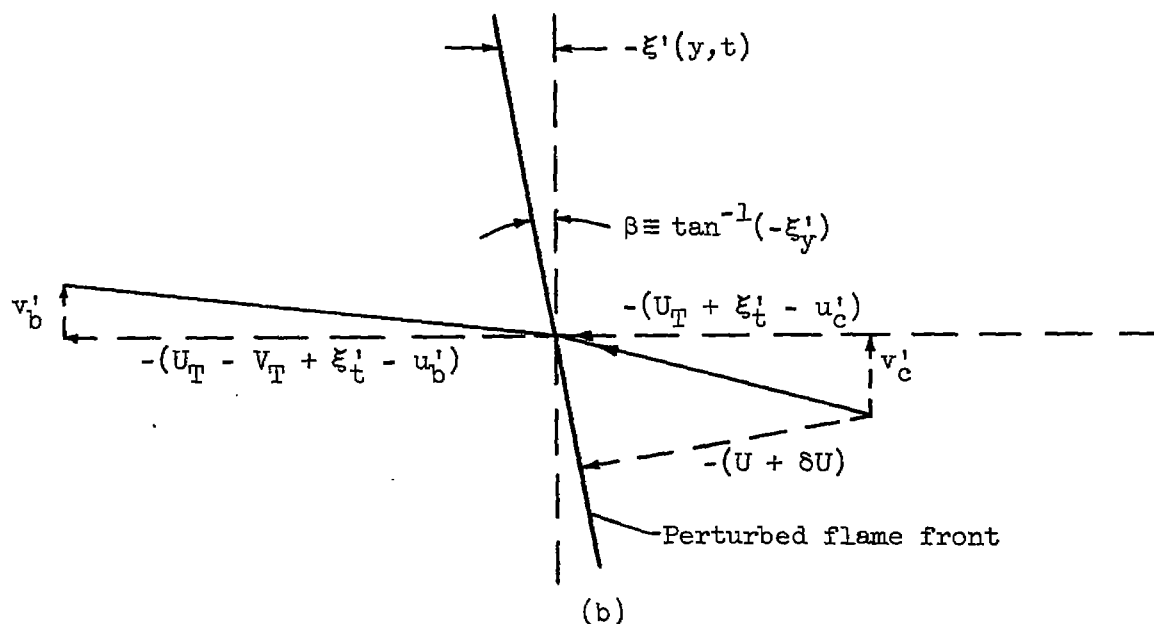
Conservation of normal and tangential momentum, energy, and mass-flow rate provide the following relations:

$$(p_c + p_c')(1 + \xi_y'^2) + (\rho_c + \rho_c')\left[(U_T + \xi_t' - u_c')^2 + v_c'^2\xi_y'^2 + 2(U_T + \xi_t' - u_c')v_c'\xi_y'\right]$$

$$= (p_b + p_b')(1 + \xi_y'^2) + (\rho_b + \rho_b')\left[(U_T - V_T + \xi_t' - u_b')^2 + v_b'^2\xi_y'^2 + 2(U_T - V_T + \xi_t' - u_b')v_b'\xi_y'\right] \quad (2a)$$

$$(U_T + \xi_t' - u_c')\xi_y' - v_c' = (U_T - V_T + \xi_t' - u_b')\xi_y' - v_b' \quad (2b)$$

$$(\tau + \tau')\left[\frac{\gamma R_g}{\gamma - 1}(T_c + T_c') + \frac{1}{2}(U_T + \xi_t' - u_c')^2 + \frac{1}{2}v_c'^2\right] = \frac{\gamma R_g}{\gamma - 1}(T_b + T_b') + \frac{1}{2}(U_T - V_T + \xi_t' - u_b')^2 + \frac{1}{2}v_b'^2 \quad (2c)$$

$$(\rho_c + \rho_c')(U_T + \xi_t' - u_c' + v_c'\xi_y') = (\rho_b + \rho_b')(U_T - V_T + \xi_t' - u_b' + v_b'\xi_y') \quad (2d)$$

Small-perturbation techniques are used to make the interaction problem amenable to analysis. Then, if the velocity perturbations are assumed to be small relative to the flame speed U_T and the flame-front slope ξ_y' is also assumed to be very small so that terms of second order in the fluctuation quantities may be neglected, application of the linearized state equation $\frac{p'}{p} = \frac{\rho'}{\rho} + \frac{T'}{T}$ and utilization of equations (1) permit the following boundary conditions at the flame front to be obtained from equations (2):

$$\frac{p_b'}{p_b} + B_1\frac{\rho_b'}{\rho_b} + B_2\frac{\xi_t' - u_b'}{U} = B_3\frac{p_c'}{p_c} + B_2\frac{\xi_t' - u_c'}{U} \quad (3a)$$

$$\frac{v_b'}{U} = \frac{v_c'}{U} + E_1\xi_y' \quad (3b)$$

$$\frac{p_b'}{p_b} - \frac{\rho_b'}{\rho_b} + K_1\frac{\xi_t' - u_b'}{U} = K_2\frac{p_c'}{p_c} + K_3\tau' + K_4\frac{\xi_t' - u_c'}{U} \quad (3c)$$

$$\frac{\rho_b'}{\rho_b} + D_1\frac{\xi_t' - u_b'}{U} = \frac{\xi_t' - u_c'}{U} + \frac{1}{\gamma}\frac{p_c'}{p_c} \quad (3d)$$

where

$$B_1 \equiv \frac{\gamma U^2}{a_b^2}\left(\frac{U - V}{U}\right)^2, \quad B_2 \equiv \frac{2\gamma U^2}{a_b^2}\left(\frac{U - V}{U}\right), \quad B_3 \equiv \frac{U - V}{U}\left(\frac{U^2}{a_c^2}\right)\left(1 + \frac{a_c^2}{U^2}\right), \quad D_1 \equiv \frac{U}{U - V}, \quad E_1 \equiv \frac{-V}{U}$$

$$K_1 \equiv (\gamma - 1)\frac{U^2}{a_b^2}\left(\frac{U - V}{U}\right), \quad K_2 \equiv \frac{\gamma - 1}{\gamma}\tau\frac{a_c^2}{a_b^2}, \quad K_3 \equiv \left(\frac{c_p T_{B,c}}{U^2}\right)(\gamma - 1)\frac{U^2}{a_b^2}, \quad K_4 \equiv (\gamma - 1)\tau\frac{U^2}{a_b^2} \quad (4)$$

$$a_c^2 \equiv \gamma R_g T_c, \quad a_b^2 \equiv \gamma R_g T_b$$

It has also been assumed that the flow upstream of the flame is isentropic. It will be shown in the section Turbulent Flame Speed that $U_T = U$ is correct through first-order terms.

Another relation is required at the flame front. For the two-dimensional case under consideration, the local instantaneous normal propagation velocity $U + \delta U$ of the distorted flame front into the combustible mixture at rest (see sketch (b)) is

$$U + \delta U = \frac{U_T + \xi_t' - u_c' + v_c'\xi_y'}{\sqrt{1 + \xi_y'^2}}$$

The incremental propagation velocity δU will be determined from existing information on laminar flames. Some support for this procedure is given in reference 13. As reported therein, radiant flux-intensity measurements on laminar and turbulent propane-air flames suggest that a small surface element of a turbulent flame is chemically and physically the same as that of a corresponding laminar flame.

The propagation speed of a laminar flame is affected by both the ambient pressure and the ambient temperature. Although the functional relations have not been rigorously determined, preliminary indications are that the pressure effect is much smaller than the temperature effect. In the present analysis the local flame propagation speed is assumed to depend only upon the temperature of the combustible mixture, that is,

$$\delta U = \frac{dU}{dT_c}\, dT_c = \left(\frac{dU}{dT_c}\right)T_c'$$

With the empirical relation obtained in reference 14 as a guide, it is assumed that $U = r_1 + r_2 T_c^n$ where r_1, r_2, and n are constants which depend upon the fuel and oxidant under consideration. Thus,

$$\delta U = nr_2 T_c^n\left(\frac{T_c'}{T_c}\right) = nr_2\left(\frac{\gamma - 1}{\gamma}\right)T_c^n\left(\frac{p_c'}{p_c}\right) \equiv U\Lambda\,\frac{p_c'}{p_c}$$

and

$$U\left(1 + \Lambda\,\frac{p_c'}{p_c}\right)\sqrt{1 + \xi_y'^2} = U_T + \xi_t' - u_c' + v_c'\xi_y'$$

Correct through first-order terms wherein $U_T = U$, the following boundary condition is obtained at the flame front:

$$\frac{\xi'_t - u'_c}{U} = \Lambda \frac{p'_c}{p_c} \tag{3e}$$

In a coordinate system fixed in space, the equations of motion for the two-dimensional fluctuation quantities in the burned gas with terms of second order neglected, are

$$\frac{\partial u'_b}{\partial t} + V \frac{\partial u'_b}{\partial x_c} = - \frac{1}{\rho_b} \frac{\partial p'_b}{\partial x_c}$$

$$\frac{\partial v'_b}{\partial t} + V \frac{\partial v'_b}{\partial x_c} = - \frac{1}{\rho_b} \frac{\partial p'_b}{\partial y}$$

$$\frac{\partial \rho'_b}{\partial t} + V \frac{\partial \rho'_b}{\partial x_c} + \rho_b \left(\frac{\partial u'_b}{\partial x_c} + \frac{\partial v'_b}{\partial y} \right) = 0$$

$$\rho_b c_v \frac{\partial T'_b}{\partial t} + \rho_b c_v V \frac{\partial T'_b}{dx_c} + p_b \left(\frac{\partial u'_b}{dx_c} + \frac{\partial v'_b}{dy} \right) = 0$$

For a coordinate system moving with constant velocity V, the preceding equations reduce to the same form as the corresponding equations for the fluctuation quantities in the combustible mixture relative to a coordinate system fixed in space. Thus, the flow equations for both the combustible-mixture fluctuations and the burned-gas fluctuations may be written, with appropriate subscripts c or b, as

$$\left. \begin{aligned} \frac{\partial u'}{\partial t} &= - \frac{1}{\rho} \frac{\partial p'}{\partial x} \\[6pt] \frac{\partial v'}{\partial t} &= - \frac{1}{\rho} \frac{\partial p'}{\partial y} \\[6pt] \frac{\partial \rho'}{\partial t} &= - \rho \left(\frac{\partial u'}{\partial x} + \frac{\partial v'}{\partial y} \right) \\[6pt] \rho c_v \frac{\partial T'}{\partial t} &= - p \left(\frac{\partial u'}{\partial x} + \frac{\partial v'}{\partial y} \right) \end{aligned} \right\} \tag{5}$$

The coordinate systems x_c, y and x_b, y for the first-order analysis are indicated in sketch (c).

(c)
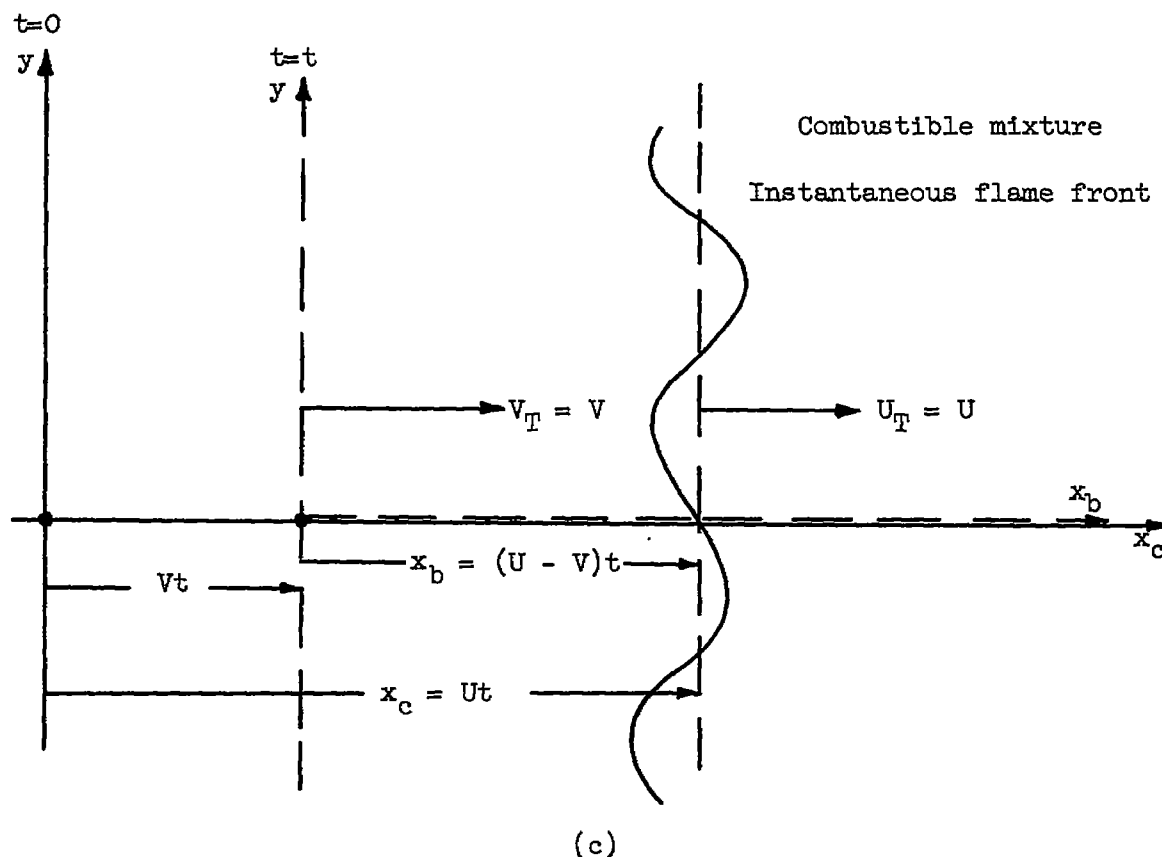
A two-dimensional vorticity wave in the combustible mixture with velocity vector of magnitude A and having its wave-number vector $\underline{k}$ inclined at an angle φ to the positive direction of the x_c-axis may be written in the form

$$\frac{u'_{s,c}}{U} = (A \sin \varphi)e^{i\nu}, \quad \frac{v'_{s,c}}{U} = (- A \cos \varphi)e^{i\nu}$$

where $\nu \equiv k'_1 x_c + k'_2 y$, and k'_1 and k'_2 are components of the wave-number vector $\underline{k}$ in the x_c- and the y-directions, respectively, with $k'_2/k'_1 = \tan \varphi$. As a result of the linear boundary conditions of equations (3), obtaining a unique solution of the interaction problem requires that the arguments of all disturbance waves match at the flame

front. This matching requirement together with provision for differ-
ences in phase angle yields the following form for the vorticity wave
present in the burned gas:

$$\frac{u'_{s,b}}{U} = (G_1 + iG_2)e^{i\psi}, \quad \frac{v'_{s,b}}{U} = (I_1 + iI_2)e^{i\psi}$$

where

$$\psi \equiv \frac{U}{U - V}k'_1 x_b + k'_2 y$$

Pressure fluctuations generated by the interaction must satisfy the
following wave equation, with appropriate subscripts c or b, which is
obtainable from equations (5):

$$\frac{\partial^2 p'}{\partial t^2} - a^2\left(\frac{\partial^2 p'}{\partial x^2} + \frac{\partial^2 p'}{\partial y^2}\right) = 0 \qquad (6)$$

The present analysis will be concerned with the limiting case of very
slow flow (constant-pressure combustion). It is clear from the rela-
tions given for the critical wave-inclination angles $\varphi_{cr,c}$ and $\varphi_{cr,b}$
that, for very slow flows, only the irrotational isentropic pressure
waves described in the section FLAME - TURBULENCE INTERACTION PROCESS
will be generated by the interaction. The form of these pressure waves
that satisfies equation (6) has already been established in reference 12
in terms of the variables η and ζ, where

$$\left.\begin{array}{l} \eta_c \equiv (f_c)(x_c - Ut) \\[8pt] \zeta_c \equiv b_c x_c + c_c y + Ud_c t \\[8pt] \eta_b \equiv (f_b)\left[-x_b + (U - V)t\right] \\[8pt] \zeta_b \equiv b_b x_b + c_b y + Ud_b t \end{array}\right\} \qquad (7)$$

The variable η is proportional to the distance from the flame front.
At the front, $\eta_c = \eta_b = 0$; upstream of the flame, η_c is positive; and
downstream of the flame, η_b is positive. The equation $\zeta = $ constant
defines planes moving with constant velocity $(Ud)_{c,b}$ at an angle
$\tan^{-1}(c/b)_{c,b}$ to the flame velocity U. Equation (6) takes the form
of Laplace's equation

$$\left(\frac{\partial^2}{\partial \eta^2} + \frac{\partial^2}{\partial \zeta^2}\right)\frac{p'}{p} = 0$$

when

$$\left(\frac{\partial \eta}{\partial t}\right)^2 - \left(\frac{\partial \zeta}{\partial t}\right)^2 = a^2 \left[\left(\frac{\partial \eta}{\partial x}\right)^2 - \left(\frac{\partial \zeta}{\partial x}\right)^2 - \left(\frac{\partial \zeta}{\partial y}\right)^2\right] \Bigg\}$$

$$\frac{\partial \eta}{\partial t} \frac{\partial \zeta}{\partial t} = a^2 \frac{\partial \eta}{\partial x} \frac{\partial \zeta}{\partial x}$$

(8)

Matching arguments of the pressure and vorticity waves at the combustion front where $\eta = 0$ and satisfying the requirements of equations (8) provide the following values for the constants of equation (7):

$$c_c = c_b = k_2', \quad b_c = -\frac{k_1' M^2}{1 - M^2}, \quad b_b = \frac{-k_1'\left(\frac{U - V}{U}\right)\frac{U^2}{a_b^2}}{1 - \left(\frac{U - V}{U}\right)^2 \frac{U^2}{a_b^2}}, \quad d_c = \frac{k_1'}{1 - M^2}$$

$$d_b = \frac{k_1'}{1 - \left(\frac{U - V}{U}\right)^2 \frac{U^2}{a_b^2}}, \quad f_c^2 = \frac{b_c^2 + c_c^2 - d_c^2 M^2}{1 - M^2}, \quad f_b^2 = \frac{b_b^2 + c_b^2 - d_b^2 \frac{U^2}{a_b^2}}{1 - \left(\frac{U - V}{U}\right)^2 \frac{U^2}{a_b^2}}$$

(9)

In addition to the boundary condition from equations (3), the pressure fluctuations will be required to satisfy the boundary condition $\frac{p'}{p} = 0$ at $\eta = \infty$. Utilizing equations (36) and (37) of reference 12 yields

$$\frac{p_c'}{p_c} = (R_1 + iR_2)e^{i\zeta_c - \eta_c}$$

(10a)

$$\frac{p_b'}{p_b} = (J_1 + iJ_2)e^{i\zeta_b - \eta_b}$$

(10b)

In the combustible mixture, density fluctuations are associated only with the pressure fluctuations according to the isentropic relation $\frac{\rho_c'}{\rho_c} = \frac{1}{\gamma}\frac{p_c'}{p_c}$. In the burned gas, density fluctuations may also be caused by entropy fluctuations generated by flame distortion and heat-release fluctuations, if present, as well as by pressure fluctuations. Velocity

fluctuations are associated with both pressure fluctuations and vorticity fluctuations. It is convenient to deal with the pressure coefficient $\frac{p'}{\rho_c U^2}$. Thus, the disturbances arising from the interaction of the flame front and incident vorticity wave take the following forms:

$$\frac{p'_c}{\rho_c U^2} = \frac{1}{\gamma M^2}\,(R_1 + iR_2)e^{i\zeta_c - \eta_c} \equiv \left(R^{(1)} + iR^{(2)}\right)e^{i\zeta_c - \eta_c} \tag{10c}$$

$$\frac{p'_b}{\rho_c U^2} = \frac{p_b}{\rho_c U^2}\,(J_1 + iJ_2)e^{i\zeta_b - \eta_b} \equiv \left(J^{(1)} + iJ^{(2)}\right)e^{i\zeta_b - \eta_b} \tag{10d}$$

$$\frac{\rho'_b}{\rho_b} = \frac{1}{\gamma}\,(J_1 + iJ_2)e^{i\zeta_b - \eta_b} + (L_1 + iL_2)e^{i\psi} \tag{10e}$$

$$\frac{u'_b}{U} = (N_1 + iN_2)e^{i\zeta_b - \eta_b} + (G_1 + iG_2)e^{i\psi} \tag{10f}$$

$$\frac{v'_b}{U} = (P_1 + iP_2)e^{i\zeta_b - \eta_b} + (I_1 + iI_2)e^{i\psi} \tag{10g}$$

$$\frac{u'_c}{U} = (W_1 + iW_2)e^{i\zeta_c - \eta_c} + (A\sin\varphi)e^{i\nu} \tag{10h}$$

$$\frac{v'_c}{U} = (X_1 + iX_2)e^{i\zeta_c - \eta_c} - (A\cos\varphi)e^{i\nu} \tag{10i}$$

The flame displacement velocity may be written

$$\frac{\xi'_t}{U} = (H_1 + iH_2)e^{i(k'_1 Ut + k'_2 y)} \equiv (H_1 + iH_2)e^{i\sigma} \tag{10j}$$

To satisfy the requirements that the arguments of all disturbance quantities match at the flame front and that $\frac{\partial^2 \xi}{\partial t\,\partial y} = \frac{\partial^2 \xi}{\partial y\,\partial t}$, the flame-front slope must take the form

$$\xi'_y = (H_1 + iH_2)(\tan\varphi)e^{i\sigma} \tag{10k}$$

Integration of equation (10j) with respect to time t gives the flame displacement as

$$\xi' = \frac{1}{k_1'} (H_2 - iH_1)e^{i\sigma} = \frac{\tan \varphi}{k_2'} (H_2 - iH_1)e^{i\sigma} \qquad (10l)$$

Extension to Three-Dimensional Disturbances

Equations (10) describe the interaction of a flame front with a constant-density vorticity wave having velocity components

$$\frac{u_{s,c}'}{U} = (A \sin \varphi)e^{i\nu} \quad \text{and} \quad \frac{v_{s,c}'}{U} = (- A \cos \varphi)e^{i\nu}$$

in the x_c- and y-directions, respectively. The vorticity wave may be considered to have a third velocity component $\dfrac{w_{s,c}'}{U} = Ce^{i\nu}$ in the z-direction. In the preceding linearized analysis, the amplitude C was not prescribed. This component, which is normal to both the u' and v' components and parallel to the plane of the flame front, then is associated with a corresponding component of the vorticity wave in the burned gas $\dfrac{w_{s,b}'}{U} = Ce^{i\psi}$.

Inasmuch as turbulence fields are three-dimensional, the interaction equations must be revised accordingly for application to the spectral analysis which follows. Assume, as shown in sketch (d), that the polarization plane which will contain the wave-number vector $\underline{k}$ is inclined at some angle θ to the $x_{1,c}$, $x_{2,c}$-plane of a new coordinate system $x_{1,c}$, $x_{2,c}$, $x_{3,c}$ fixed in space for the combustible mixture.

(d)

3493
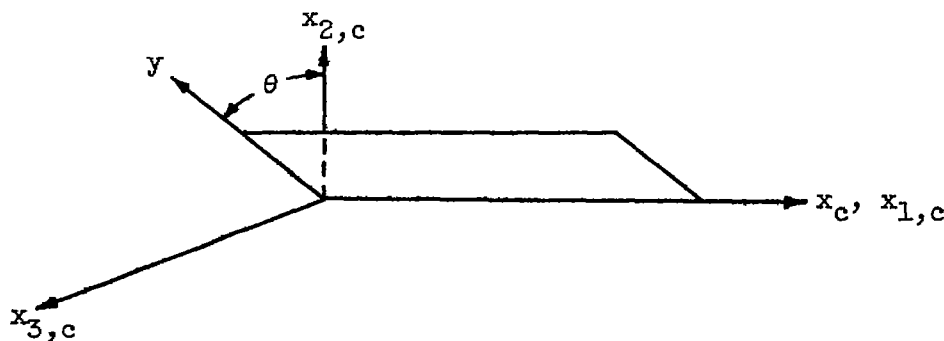
The corresponding coordinate system $x_{1,b}$, $x_{2,b}$, $x_{3,b}$ for the burned gas is assumed to be moving with mean-flow velocity V. Components k_1, k_2, and k_3 of the wave-number vector $\underline{k}$ in the directions of $x_{1,c}$, $x_{2,c}$, and $x_{3,c}$, respectively, are

$$\left.\begin{aligned}
k_1 &= k \cos \varphi \\
k_2 &= k \sin \varphi \cos \theta \\
k_3 &= k \sin \varphi \sin \theta
\end{aligned}\right\} \tag{11}$$

With primed perturbation vector quantities referring to the original coordinates x_c, x_b, y, z and unprimed perturbation vector quantities referring to the $x_{1,c}$, $x_{2,c}$, $x_{3,c}$ and $x_{1,b}$, $x_{2,b}$, $x_{3,b}$ coordinate systems, the following transformation relations apply:

$$\left.\begin{aligned}
u_{1,c} &= u_c' \qquad u_{1,b} = u_b' \\
u_{2,c} &= v_c' \cos \theta - w_c' \sin \theta \qquad u_{2,b} = v_b' \cos \theta - w_b' \sin \theta \\
u_{3,c} &= v_c' \sin \theta + w_c' \cos \theta \qquad u_{3,b} = v_b' \sin \theta + w_b' \cos \theta \\
\xi &= \xi' \\
\xi_t &= \xi_t' \\
\xi_{x_{2,c}} &= \xi_y' \cos \theta \\
\xi_{x_{3,c}} &= \xi_y' \sin \theta
\end{aligned}\right\} \tag{12}$$

This notation refers only to equation (12).

With the use of equations (10) and (12), the interaction fluctuation quantities (again designated by primes) referred to the coordinate axes $x_{1,c}$, $x_{2,c}$, $x_{3,c}$ and $x_{1,b}$, $x_{2,b}$, $x_{3,b}$ may be written as

$$\frac{p_c'}{\rho_c U^2} = \left(R^{(1)} + iR^{(2)}\right)e^{i\zeta_c - \eta_c}$$

$$\frac{p_b'}{\rho_c U^2} = \left(J^{(1)} + iJ^{(2)}\right)e^{i\zeta_b - \eta_b}$$

$$\frac{\rho_c'}{\rho_c} = \frac{1}{\gamma}(R_1 + iR_2)e^{i\zeta_c - \eta_c}$$

$$\frac{\rho_b'}{\rho_b} = \frac{1}{\gamma}(J_1 + iJ_2)e^{i\zeta_b - \eta_b} + (L_1 + iL_2)e^{i\psi}$$

$$\frac{u_{1,c}'}{U} = (W_1 + iW_2)e^{i\zeta_c - \eta_c} + (A\sin\varphi)e^{i\nu}$$

$$\frac{u_{2,c}'}{U} = (X_1 + iX_2)(\cos\theta)e^{i\zeta_c - \eta_c} - (A\cos\varphi\cos\theta + C\sin\theta)e^{i\nu}$$

$$\frac{u_{3,c}'}{U} = (X_1 + iX_2)(\sin\theta)e^{i\zeta_c - \eta_c} - (A\cos\varphi\sin\theta - C\cos\theta)e^{i\nu}$$

$$\frac{u_{1,b}'}{U} = (N_1 + iN_2)e^{i\zeta_b - \eta_b} + (G_1 + iG_2)e^{i\psi}$$

$$\frac{u_{2,b}'}{U} = (P_1 + iP_2)(\cos\theta)e^{i\zeta_b - \eta_b} + \left[(I_1 + iI_2)\cos\theta - C\sin\theta\right]e^{i\psi}$$

$$\frac{u_{3,b}'}{U} = (P_1 + iP_2)(\sin\theta)e^{i\zeta_b - \eta_b} + \left[(I_1 + iI_2)\sin\theta + C\cos\theta\right]e^{i\psi}$$

$$\frac{\xi_t'}{U} = (H_1 + iH_2)e^{i\sigma}$$

$$\xi_{x_2,c}' = (H_1 + iH_2)(\tan\varphi\cos\theta)e^{i\sigma}$$

$$\xi_{x_3,c}' = (H_1 + iH_2)(\tan\varphi\sin\theta)e^{i\sigma}$$

$$\xi' = \frac{(H_2 - iH_1)e^{i\sigma}}{k_1'}$$

(13)

The fluctuation amplitude coefficients of equations (10) or (13) may be determined from equations (3) and (5). Details of the solution are given in appendixes B and C. The general solution for the attenuating pressure-wave regime is indicated in appendix B. Inasmuch as the flame Mach number $M \equiv \dfrac{U}{a_c}$ is generally much less than 0.01, the limiting case of very slow flow (constant-pressure combustion) provides a reasonable simplification of the problem and only the attenuating-wave solution need be considered. The amplitude coefficients for this limiting case are given in appendix C (eqs. (C8)).

Equations (13) and (C8) describe the linearized interaction of a constant-pressure flame front with a single vorticity wave or shear wave having its wave-number vector $\underline{k}$ inclined at an angle φ to the direction of travel of the undisturbed flame front and having its plane of polarization inclined at an angle θ to the $x_{1,c}$, $x_{2,c}$-plane of the coordinate axes $x_{1,c}$, $x_{2,c}$, $x_{3,c}$. The wave-number vector of the shear wave generated in the burned gas makes an angle $\varphi_b \doteq \tan^{-1}(\tau \tan \varphi)$ with the direction of propagation of the undisturbed flame front. Attenuating potential fields are generated in both the combustible mixture and the burned gas. Physical quantities associated with these fields attenuate exponentially with increasing distance from the flame front. The amplitude coefficients for a given heat release (a prescribed τ), a given inclination angle φ and polarization angle θ depend upon both the intensity of the incident vorticity wave and the heat-release perturbation parameter τ'/τ. In the absence of such heat-release perturbations, there are no density fluctuations in the burned gas (correct to order M^2).

These single-wave results may be used to determine the interaction of a constant-pressure combustion front with a turbulence field of constant density for the case of negligible turbulence decay. The turbulence field will contain an infinite number of transverse plane waves with all wave lengths and planes of polarization. The spectral analysis technique used in obtaining such a superposition of waves will be discussed briefly before proceeding with the interaction problem.

SPECTRAL ANALYSIS.

General Considerations

A turbulence field satisfying the incompressible-flow continuity equation may be represented by the following superposition of plane transverse waves:

$$\underline{u}(\underline{x},t) = \int\!\!\int_{-\infty}^{\infty}\!\!\int e^{i\underline{k}\cdot\underline{x}}\underline{dZ}(\underline{k},t)$$

where $\underline{x}$ is a position vector, $\underline{k}$ is a wave-number vector, t is the time, and $\underline{dZ}(\underline{k},t)$ is the random amplitude vector of a component wave; and the subscript i takes on the values 1, 2, and 3. The quantity $\underline{dZ}(\underline{k},t)e^{i\underline{k}\cdot\underline{x}}$ represents the contribution to the velocity field from a volume element $d\underline{k}$ in wave-number space. When, as in the present case, the equations of motion are linear there is no modulation or interference between component waves, and the various statistical quantities describing a random field may be obtained from the results of a single-wave analysis. To avoid the interpretative difficulties associated with the random variable $\underline{Z}(\underline{k},t)$, which is nondifferentiable with respect to $\underline{k}$, use is made of the techniques of references 10 and 15 which utilize correlation spectra rather than amplitude spectra in the analysis of homogeneous turbulence.

A velocity correlation is defined as the ensemble average $\overline{u_i(\underline{x},t)u_j(\underline{x}',t)}$ of the product of a fluctuation-velocity component u_i at $\underline{x}$ and a component u_j at $\underline{x}' = \underline{x} + \underline{r}$ where $\underline{r}$ is a separation vector. The ensemble average, designated by a bar, may be regarded as the result of averaging the product $u_i(\underline{x},t)u_j(\underline{x},t)$ at a given instant over a very large number of statistically similar fields. The nine velocity correlations $\overline{u_i u_j}$ constitute the velocity correlation tensor $T_{ij}(\underline{x},\underline{x}',t)$. For a homogeneous field, T_{ij} depends only on $\underline{r}$, so that the tensor may be written $T_{ij}(\underline{r},t)$.

As shown in references 10 and 15, the velocity correlation tensor has the following Fourier integral expansion:

$$T_{ij}(\underline{r},t) = \int\!\!\int_{-\infty}^{\infty}\!\!\int e^{i(\underline{k}\cdot\underline{r})} dF_{ij}(\underline{k},t) = \int\!\!\int_{-\infty}^{\infty}\!\!\int e^{i(\underline{k}\cdot\underline{r})}\Phi_{ij}(\underline{k},t)d\underline{k} \tag{14}$$

where $F_{ij}(\underline{k},t)$ is the spectral tensor function, $\Phi_{ij}(\underline{k},t)$ is the spectral tensor density of a homogeneous turbulence field and

$$\Phi_{ij}(\underline{k},t)d\underline{k} = \overline{dZ_i^*(\underline{k},t)dZ_j(\underline{k},t)} \tag{15}$$

where $dZ_i^*(\underline{k},t)$ denotes the complex conjugate of $dZ_i(\underline{k},t)$. For $r = 0$ and $i = j$, equation (14) may be written

$$T_{ii}(0,t) = \overline{u_i^2} = \iiint\limits_{-\infty}^{\infty} \overline{dZ_i^*(\underline{k},t)dZ_i(\underline{k},t)} \qquad (16)$$

For homogeneous turbulence fields, wherein ensemble averages and space averages are identical, equations (15) and (16) provide the basis for obtaining the spatial mean-square velocity components from the single-wave results given by equations (13) and (C8). Equations (15) and (16) are also applicable to scalar fields. In the absence of viscosity, as postulated, the shear-velocity fields present in the combustible mixture and in the burned gas are homogeneous and application of equation (16) presents no complications. The corresponding potential-flow fields, although spatially inhomogeneous, are homogeneous in the given x_2,x_3-planes. It has been shown in reference 16 that equation (16), in effect, may be applied for such fields to obtain the mean-square fluctuations pertaining to a given plane of homogeneity.

As a result of the preceding discussion, the single-wave interaction results for constant-pressure combustion will be used to obtain the spectral densities of the fluctuation quantities at the flame front where the attenuation factors $e^{-\eta_c}$ and $e^{-\eta_b}$ are unity and $\zeta_c = \zeta_b = \sigma = \psi = \nu$. For conciseness define $RA \sin \varphi \equiv R^{(1)} + iR^{(2)}$, $WA \sin \varphi \equiv W_1 + iW_2$, $GA \sin \varphi \equiv G_1 + iG_2$, $NA \sin \varphi \equiv N_1 + iN_2$, $HA \sin \varphi \equiv H_1 + iH_2$, and $C^1 A \sin \varphi \equiv C$. With the notation

$$\overline{u_{1,s,c}^2} \equiv \iiint\limits_{-\infty}^{\infty} \overline{dZ_{1,c}^* dZ_{1,c}}$$

and, for example,

$$\overline{\left(\frac{p_c'}{\rho_c U^2}\right)^2} \equiv \iiint\limits_{-\infty}^{\infty} \overline{d\left(\frac{p_c'}{\rho_c U^2}\right)^* d\left(\frac{p_c'}{\rho_c U^2}\right)}$$

as in equation (16), the following equations are obtained by analogy with equations (13) and (C8) for the case where heat-release perturbations are absent, that is, $\tau' = 0$:

$$d\left(\frac{p'_c}{\rho_c U^2}\right) = d\left(\frac{p'_b}{\rho_c U^2}\right) = R\ dZ_{1,c}$$

$$d\left(\frac{u'_{1,c}}{U}\right) = W\ dZ_{1,c} + dZ_{1,c}$$

$$d\left(\frac{u'_{2,c}}{U}\right) = -\ iW \cos\theta\ dZ_{1,c} - (\cot\varphi\cos\theta + C^1\sin\theta)dZ_{1,c}$$

$$d\left(\frac{u'_{3,c}}{U}\right) = -\ iW \sin\theta\ dZ_{1,c} - (\cot\varphi\sin\theta - C^1\cos\theta)dZ_{1,c}$$

$$d\left(\frac{u'_{1,b}}{U}\right) = N\ dZ_{1,c} + G\ dZ_{1,c}$$

$$d\left(\frac{u'_{2,b}}{U}\right) = iN\cos\theta\ dZ_{1,c} - \left(\frac{\cot\varphi\cos\theta}{\tau}G + C^1\sin\theta\right)dZ_{1,c}$$

$$d\left(\frac{u'_{3,b}}{U}\right) = iN\sin\theta\ dZ_{1,c} - \left(\frac{\cot\varphi\sin\theta}{\tau}G - C^1\cos\theta\right)dZ_{1,c}$$

$$d(\xi') = -\frac{iH}{k'_1}dZ_{1,c} = -\frac{iH}{k\cos\varphi}dZ_{1,c}$$

$$d\left(\frac{\xi_t}{U}\right) = H\ dZ_{1,c}$$

$$d\left(\xi'_{x_{2,c}}\right) = H\tan\varphi\cos\theta\ dZ_{1,c}$$

$$d\left(\xi'_{x_{3,c}}\right) = H\tan\varphi\sin\theta\ dZ_{1,c}$$

$$\left.\right\} \quad (17)$$

In the velocity ratios of equations (17), the first term on the right side represents the potential-flow contributions $\frac{u_{i,p,c}}{U}$ or $\frac{u_{i,p,b}}{U}$; the second term represents the shear-flow contributions $\frac{u_{i,s,c}}{U}$ or $\frac{u_{i,s,b}}{U}$. The subscript i takes on the values 1, 2, and 3.

At a given instant the spatial mean-square potential- and shear-flow contributions of the disturbance fields are obtained from equations (17):

$$\overline{\left(\frac{p_c'}{\rho_c U^2}\right)^2} = \overline{\left(\frac{p_b'}{\rho_c U^2}\right)^2} = \iiint_{-\infty}^{\infty} (R^*R)\ \overline{dZ_{1,c}^* dZ_{1,c}}$$

$$\overline{\left(\frac{u_{1,s,c}}{U}\right)^2} = \iiint_{-\infty}^{\infty} \overline{dZ_{1,c}^* dZ_{1,c}}$$

$$\overline{\left(\frac{u_{2,s,c}}{U}\right)^2} + \overline{\left(\frac{u_{3,s,c}}{U}\right)^2} = \iiint_{-\infty}^{\infty} \overline{dZ_{2,c}^* dZ_{2,c}} + \overline{dZ_{3,c}^* dZ_{3,c}}$$

$$\overline{\left(\frac{u_{1,p,c}}{U}\right)^2} = \overline{\left(\frac{u_{2,p,c}}{U}\right)^2} + \overline{\left(\frac{u_{3,p,c}}{U}\right)^2} = \iiint_{-\infty}^{\infty} (W^*W)\ \overline{dZ_{1,c}^* dZ_{1,c}}$$

$$\overline{\left(\frac{u_{1,s,b}}{U}\right)^2} = \iiint_{-\infty}^{\infty} (G^*G)\ \overline{dZ_{1,c}^* dZ_{1,c}}$$

$$\overline{\left(\frac{u_{2,s,b}}{U}\right)^2} + \overline{\left(\frac{u_{3,s,b}}{U}\right)^2} = \overline{\left(\frac{u_{2,s,c}}{U}\right)^2} + \overline{\left(\frac{u_{3,s,c}}{U}\right)^2} + \iiint_{-\infty}^{\infty} \left(\frac{\cot\varphi}{\tau}\right)^2 (G^*G - \tau)^2\ \overline{dZ_{1,c}^* dZ_{1,c}}$$

$$\overline{\left(\frac{u_{1,p,b}}{U}\right)^2} = \overline{\left(\frac{u_{2,p,b}}{U}\right)^2} + \overline{\left(\frac{u_{3,p,b}}{U}\right)^2} = \iiint_{-\infty}^{\infty} (N^*N)\ \overline{dZ_{1,c}^* dZ_{1,c}}$$

(18)

The mean-square flame front quantities are

$$\overline{\left(\frac{\xi_t}{U}\right)^2} = \iiint_{-\infty}^{\infty} (H^*H)\ \overline{dZ_{1,c}^* dZ_{1,c}}$$

$$\overline{\xi^2} = \iiint_{-\infty}^{\infty} \frac{(H^*H)}{k^2\cos^2\varphi}\ \overline{dZ_{1,c}^* dZ_{1,c}}$$

$$\overline{\xi_{x_{2,c}}^2} + \overline{\xi_{x_{3,c}}^2} = \iiint_{-\infty}^{\infty} (H^*H)\ \tan^2\varphi\ \overline{dZ_{1,c}^* dZ_{1,c}}$$

From equations (C8) of appendix C, with $\tau' = 0$:

$$R^*R = \frac{(\tau - 1)^2(\tau \tan^2\varphi - 1)^2}{\Delta \sin^2\varphi}$$

$$W^*W = \frac{(\tau - 1)^2(\tau \tan^2\varphi - 1)^2}{\Delta}$$

$$G^*G = \frac{\tau^2\sec^2\varphi\left[\Delta - 4\tau(\tau^2 - 1)\tan^2\varphi\right]}{\Delta(1 + \tau^2\tan^2\varphi)}$$

$$N^*N = \frac{\tau^2(\tau - 1)^2(\tau \tan^2\varphi - 1)^2\sec^2\varphi}{\Delta(1 + \tau^2\tan^2\varphi)}$$

$$H^*H = \frac{4\tau^2\sec^2\varphi}{\Delta}$$

(19)

Mean-Square Fluctuations for Initial Isotropic Turbulence

For a given combustion process (τ and U prescribed), the spatial mean-square fluctuations of equations (18) depend upon the quantity $\overline{dZ^*_{1,c}dZ_{1,c}}$, which is specified by the type of turbulence present in the combustible mixture. The results obtained in reference 16 for the interaction of axisymmetric turbulence with a shock wave suggest that for the present problem the degree of anisotropy of the incident turbulence field may not be critical. For simplicity, the turbulence in the combustible mixture is assumed isotropic.

As indicated in reference 10, the spectral density tensors for any isotropic turbulence field satisfying the incompressible-flow continuity equation are

$$\Phi_{ij}(\underline{k}) = \mathfrak{L}(k)(k^2\delta_{ij} - k_ik_j) \tag{20}$$

where $k^2 = k_1^2 + k_2^2 + k_3^2$; $\delta_{ij} = 1$ for $i = j$; and $\delta_{ij} = 0$ for $i \neq j$; and $\mathfrak{L}(k)$ is the scalar amplitude function defining the spectral density tensor. From equations (15), (20), and (11),

$$\overline{dZ^*_{1,c}dZ_{1,c}} = \mathfrak{L}(k)k^2\sin^2\varphi \, d\underline{k}$$

or, transforming to spherical polar coordinates k, θ, φ, wherein $d\underline{k} \equiv dk_1 dk_2 dk_3 = k^2 \sin\varphi\, dk\, d\theta\, d\varphi$, yields

$$
\left.
\begin{aligned}
\overline{dZ^*_{1,c} dZ_{1,c}} &= \Omega(k)k^4 dk\, d\theta\, \sin^3\varphi\, d\varphi \\[2mm]
\overline{dZ^*_{2,c} dZ_{2,c}} &= \Omega(k)k^4 dk\, d\theta\, \sin\varphi\left[\cos^2\varphi + \sin^2\varphi\, \sin^2\theta\right]d\varphi \\[2mm]
\overline{dZ^*_{3,c} dZ_{3,c}} &= \Omega(k)k^4 dk\, d\theta\, \sin\varphi\left[\cos^2\varphi + \sin^2\varphi\, \cos^2\theta\right]d\varphi \\[2mm]
\overline{dZ^*_{2,c} dZ_{2,c}} + \overline{dZ^*_{3,c} dZ_{3,c}} &= \Omega(k)k^4 dk\, d\theta\, \sin\varphi\left[1 + \cos^2\varphi\right]d\varphi
\end{aligned}
\right\} \quad (21)
$$

The mean-square velocity components of the incident isotropic turbulence field are then given by

$$
\left.
\begin{aligned}
\overline{\left(\frac{u_{1,s,c}}{U}\right)^2} &= \int_0^\infty \Omega(k)k^4 dk \int_0^{2\pi} d\theta \int_0^{\pi} \sin^3\varphi\, d\varphi = \frac{8\pi}{3}\int_0^\infty \Omega(k)k^4 dk \\[3mm]
\overline{\left(\frac{u_{2,s,c}}{U}\right)^2} + \overline{\left(\frac{u_{3,s,c}}{U}\right)^2} &= \int_0^\infty \Omega(k)k^4 dk \int_0^{2\pi} d\theta \int_0^{\pi} \sin\varphi(1 + \cos^2\varphi)d\varphi \\[3mm]
&= \frac{16\pi}{3}\int_0^\infty \Omega(k)k^4 dk
\end{aligned}
\right\}
$$

$$(22)$$

The remaining spatial mean-square fluctuation quantities, referred to the intensities of equations (22) in order that the scale need not be specified, are given by

$$
\frac{\overline{\left(\dfrac{p'_c}{\rho_c U^2}\right)^2}}{\overline{\left(\dfrac{u_{1,s,c}}{U}\right)^2}} = \frac{\overline{\left(\dfrac{p'_b}{\rho_c U^2}\right)^2}}{\overline{\left(\dfrac{u_{1,s,c}}{U}\right)^2}} = \frac{3}{4}(\tau - 1)^2 \int_0^{\pi} \frac{\sin\varphi}{\Delta}(\tau \tan^2\varphi - 1)^2 d\varphi
$$

$$(23a)$$

$$\frac{\overline{\left(\dfrac{u_{1,p,c}}{U}\right)^2}}{\overline{\left(\dfrac{u_{1,s,c}}{U}\right)^2}} = \frac{\overline{\left(\dfrac{u_{2,p,c}}{U}\right)^2} + \overline{\left(\dfrac{u_{3,p,c}}{U}\right)^2}}{\overline{\left(\dfrac{u_{1,s,c}}{U}\right)^2}} = \frac{3}{4}(\tau-1)^2 \int_0^\pi \frac{\sin^3\varphi}{\Delta}(\tau\,\tan^2\varphi-1)^2\,d\varphi$$

(23b)

$$\frac{\overline{\left(\dfrac{u_{1,s,b}}{U}\right)^2}}{\overline{\left(\dfrac{u_{1,s,c}}{U}\right)^2}} = \frac{3\tau^2}{4} \int_0^\pi \frac{\left[\Delta - 4\tau(\tau^2-1)\tan^2\varphi\right]\sin\varphi\,\tan^2\varphi}{\Delta(1+\tau^2\tan^2\varphi)}\,d\varphi \qquad (23c)$$

$$\frac{\overline{\left(\dfrac{u_{2,s,b}}{U}\right)^2} + \overline{\left(\dfrac{u_{3,s,b}}{U}\right)^2}}{\overline{\left(\dfrac{u_{2,s,c}}{U}\right)^2} + \overline{\left(\dfrac{u_{3,s,c}}{U}\right)^2}} = 1 - \frac{3}{8}(\tau^2-1) \int_0^\pi \frac{\left[\Delta + 4\tau\,\sec^2\varphi\right]\sin^3\varphi}{\Delta\left[1+\tau^2\tan^2\varphi\right]}\,d\varphi$$

(23d)

$$\frac{\overline{\left(\dfrac{u_{1,p,b}}{U}\right)^2}}{\overline{\left(\dfrac{u_{1,s,c}}{U}\right)^2}} = \frac{\overline{\left(\dfrac{u_{2,p,b}}{U}\right)^2} + \overline{\left(\dfrac{u_{3,p,b}}{U}\right)^2}}{\overline{\left(\dfrac{u_{1,s,c}}{U}\right)^2}} = \frac{3}{4}\tau^2(\tau-1)^2 \int_0^\pi \frac{(\tau\,\tan^2\varphi-1)^2\sin\varphi\,\tan^2\varphi}{\Delta\left[1+\tau^2\tan^2\varphi\right]}\,d\varphi \qquad (23e)$$

$$\frac{\overline{\left(\dfrac{\xi_t}{U}\right)^2}}{\overline{\left(\dfrac{u_{1,s,c}}{U}\right)^2}} = 3\tau^2 \int_0^\pi \frac{\sin\varphi\,\tan^2\varphi}{\Delta}\,d\varphi \qquad (23f)$$

$$\frac{\overline{\xi^2_{x_{2,c}}} + \overline{\xi^2_{x_{3,c}}}}{\overline{\left(\dfrac{u_{1,s,c}}{U}\right)^2}} = 3\tau^2 \int_0^\pi \frac{\tan^4\varphi\,\sin\varphi}{\Delta}\,d\varphi \qquad (23g)$$

$$\frac{\overline{\xi^2}}{\left(\dfrac{u_{1,s,c}}{U}\right)^2} = 3\tau^2 \left[\frac{\displaystyle\int_0^\infty \mathfrak{Q}(k)k^2\,dk}{\displaystyle\int_0^\infty \mathfrak{Q}(k)k^4\,dk}\right] \int_0^\pi \frac{\sin^3\varphi}{\Delta\,\cos^4\varphi}\,d\varphi \qquad (23h)$$

The subscript 1 designates a longitudinal component; subscripts 2 and 3 designate the lateral components. Of the remaining subscripts, s denotes a shear-flow component; p denotes a potential-flow component; c refers to the combustible mixture; and b refers to the burned gas. Equations (23a) to (23g) have been integrated numerically using Simpson's rule with the following increments for φ: 2° intervals from 0° to 20°, 5° intervals from 20° to 70°, 2° intervals from 70° to 90°, and so forth. Numerical results are listed in table I.

DISCUSSION OF RESULTS

Mean-square fluctuation quantities generated by the linearized interaction of a constant-pressure combustion front with a weak isotropic turbulence field satisfying the continuity equation for incompressible flow are given by equations (23) in terms of the incident-turbulence-velocity components. Equations (23a), (23b), and (23e) apply only at the flame front where the attenuation factors are unity. This restriction does not apply to equations (23c) and (23d) in the assumed absence of turbulent decay processes.

Velocity Fluctuations

Potential-flow fluctuations. - The root-mean-square velocities associated with the attenuating pressure fields generated in the combustible mixture (eq. (23b)) and in the burned gas (eq. (23e)) are plotted in figure 2. Since these ratios apply only at the flame front where the exponential attenuation factors are unity, they represent maximum values. As is to be expected from the boundary-condition requirement of equal pressure fluctuations with differing densities on each side of' the flame front, potential-flow velocity components in the burned gas exceed those in the combustible mixture. Both ratios increase with increasing flame-temperature ratio, reaching asymptotic values of $\sqrt{3/2}$ in the burned gas and unity in the combustible mixture. Hot-wire instrumentation will respond to these fluctuation velocities as well as to the shear-flow fluctuation velocities. In view of their exponential attenuation characteristics, however, such contributions would not be of importance unless measurements were made at stations very close to the flame, that is, within a distance of the order of

incident-turbulence scale. For the low flame Mach numbers encountered
in combustion, the contribution to the hot-wire signal voltage of the
unattenuated sound waves described in the section FLAME - TURBULENCE
INTERACTION PROCESS should be quite small.

Flame-generated turbulence. - The shear flow in the burned gas
(eqs. (23c) and (23d)) constitutes the flame-generated turbulence oc-
casioned by the presence of approach-flow turbulence. These velocities,
referred to the incident turbulence velocities, are also plotted in fig-
ure 2. A slight amplification of the longitudinal component occurs for
values of τ in excess of 7. In the limit, as τ becomes very large
the longitudinal and lateral velocity ratios approach asymptotic values
of $\sqrt{3/2}$ and $\frac{1}{2} \sqrt{3}$, respectively.

The diagrams of figure 1 indicate that a pressure wave interacting
with the flame front can also bring about a shear flow in the burned
gas. Although the reflection and the consequent impingement of the
pressure fields described by equation (23a) upon the flame front are
possible, any additions to the flame-generated turbulence level through
the reflection process would probably be negligible because of the at-
tenuating nature of the pressure field. Thus, contrary to the predic-
tions of references 6 and 7 that the flame-generated turbulence inten-
sity should be many times greater than the intensity of the incident
field, the present analysis indicates that the two intensities are
about equal.

It is interesting to note that a stream contraction (ref. 17) in-
creases the downstream velocity of the mean flow (as does the flame
front also), while exercising a different selective effect upon an in-
cident isotropic turbulence field. For example, with a sevenfold in-
crease in the downstream velocity of the mean flow, the longitudinal
velocity ratio (in the absence of decay effects) is 1.01 for the flame
front and 0.31 for the contraction. The corresponding lateral velocity
ratios are 0.87 and 2.29, respectively.

Turbulent Flame Speed

The higher mass-flow burning rate of a turbulent flame as compared
with that of the corresponding laminar flame is generally described in
terms of a turbulent flame speed U_T. The flame-speed ratio U_T/U is
generally assumed to be equivalent to the ratio of turbulent-to-laminar
flame surface area.

Calculation of the turbulent flame speed requires consideration of
second-order terms. The local instantaneous normal propagation velocity

$U + \delta U$ of the distorted flame front into the combustible mixture at rest is

$$U + \delta U = \frac{U_T + \xi'_t - u'_{1,c} + \xi'_{x_{2,c}} u'_{2,c} + \xi'_{x_{3,c}} u'_{3,c}}{\sqrt{1 + \xi'^2_{x_{2,c}} + \xi'^2_{x_{3,c}}}} \qquad (24)$$

Let $U_T = U + U_① + U_② + \ldots$ where $U_Ⓝ$ represents a steady-state contribution to the flame speed of order N. The perturbation quantities, for example, are written as

$$\xi'_t = \xi_t^① + \xi_t^② + \ldots$$

$$u'_{1,c} = u_{1,c}^① + u_{1,c}^② + \ldots$$

The superscript on a fluctuation quantity $\xi_t^Ⓝ$ indicates the order of the perturbation. As before, $\delta U/U$ is taken as

$$\frac{\delta U}{U} = \frac{n r_2 T_c^n}{U} \frac{T'_c}{T_c} = \frac{(\gamma - 1) n r_2}{\sqrt{\gamma R_g}} T_c^{n - \frac{1}{2}} M \frac{p'_c}{\rho_c U^2} \equiv \Gamma \frac{p'_c}{\rho_c U^2}$$

Substitution of this expression into equation (24) and performing the indicated expansions yield the following relation, which is correct through second-order terms:

$$\underbrace{\Gamma\left(\frac{p_c^①}{\rho_c U^2}\right)}_{\substack{\text{first-} \\ \text{order} \\ \text{terms}}} + \underbrace{\left[\Gamma \frac{p_c^②}{\rho_c U^2} + \frac{1}{2}\left(\xi^{①2}_{x_{2,c}} + \xi^{①2}_{x_{3,c}}\right)\right]}_{\text{second-order terms}}$$

$$= \underbrace{\left(\frac{U_①}{U} + \frac{\xi_t^①}{U} - \frac{u_{1,c}^①}{U}\right)}_{\substack{\text{first-} \\ \text{order} \\ \text{terms}}} + \underbrace{\left(\frac{U_②}{U} + \frac{\xi_t^②}{U} - \frac{u_{1,c}^②}{U} + \frac{u_{2,c}^①}{U}\xi_{x_{2,c}}^① + \frac{u_{3,c}^①}{U}\xi_{x_{3,c}}^①\right)}_{\text{second-order terms}}$$

Averaging this equation yields

$$\frac{U^{(1)}}{U} = 0$$

$$\frac{U^{(2)}}{U} = \Gamma\,\frac{\overline{p_c^{(2)}}}{\rho_c U^2} + \frac{1}{2}\left(\overline{\xi_{x_{2,c}}^{(1)\,2}} + \overline{\xi_{x_{3,c}}^{(1)\,2}}\right) - \overline{\frac{u_{2,c}^{(1)}}{U}\,\xi_{x_{2,c}}^{(1)}} - \overline{\frac{u_{3,c}^{(1)}}{U}\,\xi_{x_{3,c}}^{(1)}}$$

For the limiting case of constant-pressure combustion, $\Gamma = 0$. Thus, the ratio of turbulent-to-laminar flame speeds can be written for this case as

$$\frac{U_T}{U} = 1 + \frac{1}{2}\left(\overline{\xi_{x_{2,c}}^{(1)\,2}} + \overline{\xi_{x_{3,c}}^{(1)\,2}}\right) - \left(\overline{\frac{u_{2,c}^{(1)}}{U}\,\xi_{x_{2,c}}^{(1)}} + \overline{\frac{u_{3,c}^{(1)}}{U}\,\xi_{x_{3,c}}^{(1)}}\right) \quad (25)$$

The first two terms on the right side of equation (25) represent the ratio of averaged turbulent-to-laminar flame surface area. The third term is a correlation coefficient representing the transverse-velocity-fluctuation contribution to the turbulent flame speed caused by flame-front distortion. It is interesting to note that only the transverse velocity fluctuations appear explicitly. The second term has already been determined (eq. (23g)). The third term may be obtained from equations (C8) as

$$-\overline{\frac{u_{2,c}^{(1)}}{U}\,\xi_{x_{2,c}}^{(1)}} - \overline{\frac{u_{3,c}^{(1)}}{U}\,\xi_{x_{3,c}}^{(1)}} = \frac{3\pi}{2}\int_0^A\left\{\left[\tau(\tau-1)\tan^4\varphi + (\tau^2+1)\tan^2\varphi + (\tau+1)\right]\frac{\sin^3\varphi}{\Delta} + i\right\}d\varphi \quad (26)$$

The imaginary term has not been written out inasmuch as it does not contribute to the integral. The results of the indicated integrations are listed in table I.

Equation (25) for the flame-speed ratio U_T/U may also be written in the form

$$\frac{U_T}{U} = 1 + S\,\frac{\overline{u_{1,s,c}^2}}{U^2} \quad (27)$$

where the flame-speed parameter S is obtained from the values listed in table I for equations (23g) and (26). The variation of this parameter with the flame-temperature ratio τ shown in figure 3 suggests, on the assumption that the flame-front slopes $\xi_{x_{2,c}}$ and $\xi_{x_{3,c}}$ govern contributions to the right side of equation (25), that the flame

front with the higher heat release is distorted less by a given inten-
sity of turbulence. For the degenerate case $\tau = 1$ (no heat release),
the parameter S becomes infinite.- a condition compatible with this
viewpoint.

The present analysis requires that the flame-front slopes, as well
as the other perturbation quantities, be small. The preceding discus-
sion suggests that the incremental flame-speed ratio $(U_T - U)/U$ may be
of second order as a result of this restriction to small flame-front
slopes.

Combustion Noise

The root-mean-square pressure-fluctuation coefficient $\sqrt{\overline{p_c'^2}}\big/\rho_c U^2$,
which applies directly at the flame front, is plotted in figure 4 for
the limiting case of constant-pressure combustion. The pressure fluc-
tuations are a measure of the random noise generated by the interaction
of the flame front with the incident turbulence. In acoustical measure-
ments the noise level in decibels is usually given with respect to a
reference pressure of 0.0002 dyne per square centimeter (ref. 18), which
corresponds approximately to the pressure amplitude of a plane sound
wave of minimum audible intensity at a frequency of 1000 cps. The noise
pressure level in decibels is defined by the relation

$$\text{noise pressure level} \cong 20 \log_{10}\left(\frac{\sqrt{\overline{p_c'^2}}}{0.0002}\right) = 74 + 20 \log_{10}\sqrt{\overline{p_c'^2}} \tag{28}$$

where the pressure fluctuations in the combustible mixture are given in
dynes per square centimeter.

Equations (23a) and (28) indicate that the noise level should be
particularly dependent upon flame speed. Propane-air and acetylene-
air combustion, which are characterized by a low flame speed and a
fairly high flame speed, respectively, will be considered for illus-
trative purposes. Pertinent data for these flames at maximum-flame-
speed and stoichiometric conditions for an ambient temperature of 25° C
and a pressure of 760 millimeters of mercury are given in table II. The
adiabatic equilibrium flame temperatures, at which the total enthalpy of
the fuel and oxidant equals the total enthalpy of the products of reac-
tion, were calculated using the procedure of reference 19. (Total en-
thalpy includes the chemical contributions to the internal energy.)
Flame-speed data were obtained from references 20 and 21.

If the flame-front turbulence intensity $\sqrt{\overline{u_{1,s,c}^2}}/U$ is assumed
equal to 10 percent, noise pressure levels of 59 and 81 decibels are
obtained for propane-air flames and acetylene-air flames, respectively,
under conditions for maximum laminar flame speed. At an approach-flow
velocity of 1225 centimeters per second, which is in the range of ve-
locities usually encountered in combustion experiments, the correspond-
ing intensity of the approach-flow turbulence would be about 0.3 percent
for the propane-air mixture and about 1 percent for the acetylene-air
mixture.

Thus, the pressure fluctuations generated at the flame front when
the incident turbulence is of low intensity, although small as compared
with ambient pressure, are apparently of fairly high acoustical inten-
sity for constant-pressure combustion. Because of the exponential at-
tenuation of these pressure fields, the "far-field" acoustic intensity
(the intensity at distances very far from the flame front) approaches
zero. For cases other than constant-pressure combustion, a finite
"far-field" intensity is obtained.

CONCLUDING REMARKS

The present linearized analysis has treated the interaction of a
field of isotropic turbulence with a free flame front under constant-
pressure combustion conditions with no turbulence decay processes or
heat-release fluctuations. The interaction produces an anisotropic
turbulence field in the burned gas which has axisymmetry about the
main-stream direction. Contrary to the results predicted by several
current theories of turbulent flame speed, the flame-generated turbu-
lence velocities caused by approach-flow turbulence do not differ
greatly from the turbulence velocities of the incident field.

The incremental flame-speed ratio $(U_T - U)/U$ as obtained from the
present analysis is a second-order quantity consisting of two parts:
One part represents the root-mean-square area of the turbulent flame
front; the other represents the contribution of the transverse veloc-
ity fluctuations which result from the flame-front distortion. The
flame-speed ratio U_T/U for a given level of incident-turbulence in-
tensity $\sqrt{\overline{u_{1,s,c}^2}}/U$ is found to decrease with increasing heat-release
rates (increasing values of τ).

Random pressure fluctuations generated in both the combustible mix-
ture and the burned gas, although small compared with ambient pressure,
give rise to appreciable noise levels (59 to 81 decibels) directly at

the flame front even for very moderate intensities of approach-flow turbulence (flame-front turbulence intensities of 10 percent). For the limiting case of constant-pressure combustion, the pressure waves attenuate exponentially with distance from the flame front, so that the "far-field" intensity approaches zero.

Lewis Flight Propulsion Laboratory
    National Advisory Committee for Aeronautics
        Cleveland, Ohio, January 25, 1955

APPENDIX A

SYMBOLS

The following symbols are used in this report:

A   magnitude of two-dimensional vorticity-wave velocity
                vector in combustible mixture

$\underline{A}$ two-dimensional vorticity-wave velocity vector in com-
                bustible mixture

a   speed of sound

B_1, B_2, B_3 coefficients defined in eqs. (4)

b   constant defined in eqs. (7) and (9)

C   amplitude of combustible mixture shear-wave component
                parallel to $x_{3,c}$-axis

c   constant defined in eqs. (7) and (9)

c_p specific heat at constant pressure

c_v specific heat at constant volume

D_1 $U/(U - V)$, eqs. (4)

d   constant defined in eqs. (7) and (9)

E_1 $-V/U$, eqs. (4)

$F_{ij}(\underline{k}, t)$ spectral tensor function

f   constant defined in eqs. (7) and (9)

G $(G_1 + iG_2)/A \sin \varphi$

G_1, G_2 amplitude coefficients of shear-wave longitudinal com-
                ponent in burned gas

H $(H_1 + iH_2)/A \sin \varphi$

H_1, H_2 amplitude coefficients of flame-front displacement

$h_1, h_2 \cdots h_{10}$ groupings defined in eqs. (B16)

3493

CJ-5-B

I_1, I_2 amplitude coefficients of shear-wave transverse component in burned gas

J_1, J_2 amplitude coefficients of pressure wave in burned gas

$J^{(1)}, J^{(2)}$ $J^{(1)} \equiv \dfrac{p_b}{\rho_c U^2} J_1; \quad J^{(2)} \equiv \dfrac{p_b}{\rho_c U^2} J_2,$ eq. (10d)

K_1, K_2, K_3, K_4 coefficients defined in eqs. (4)

k magnitude of wave-number vector $\underline{k}$

$\underline{k}$ wave-number vector of shear wave in combustible mixture with components k_1', k_2' in x_c,y-coordinate system, with components k_1, k_2, k_3 in $x_{1,c}$, $x_{2,c}, x_{3,c}$-coordinate system

L_1, L_2 amplitude coefficients of density associated with shear entropy wave in burned gas

M flame-front Mach number, $M \equiv U/a_c$

m^2 $a^2/\gamma U^2$, eq. (B16)

N $(N_1 + iN_2)/A \sin \varphi$

N_1, N_2 amplitude coefficients of longitudinal velocity component associated with pressure wave in burned gas

n exponent used in representation of laminar flame speed as function of combustible-mixture static temperature

P_1, P_2 amplitude coefficients of lateral velocity component associated with pressure wave in burned gas

p static pressure

p' static-pressure perturbation

Q term not contributing to the integral in eq. (26)

R $\left(R^{(1)} + R^{(2)}\right)/A \sin \varphi$

R_g gas constant

R_1, R_2 amplitude coefficients of pressure wave in combustible mixture

$R^{(1)}, R^{(2)}$ $R^{(1)} \equiv R_1/\gamma M^2$, $R^{(2)} = R_2/\gamma M^2$, eq. (10c)

r separation vector

r_1, r_2 constants used in representation of laminar flame speed as function of combustible-mixture static temperature

S flame-speed parameter, eq. (27)

T static temperature

$T_{ij}(r,t)$ velocity correlation tensor for homogeneous turbulence

T_s stagnation temperature

t time

U laminar or fundamental flame speed

U_T mean turbulent flame speed

u' longitudinal component of velocity perturbation

$u_{1,c}, u_{2,c}, u_{3,c}$ velocity perturbation components in combustible mixture parallel to $x_{1,c}$, $x_{2,c}$, $x_{3,c}$ coordinate axes, respectively

$u_{1,b}, u_{2,b}, u_{3,b}$ velocity perturbation components in burned gas parallel to $x_{1,b}$, $x_{2,b}$, $x_{3,b}$ coordinate axes, respectively

V mean velocity of burned gas

V_T mean velocity of burned gas in turbulent combustion

v' lateral component of velocity perturbation

W $(W_1 + iW_2)/A \sin \varphi$

W_1, W_2 amplitude coefficients of longitudinal velocity component associated with pressure wave in combustible mixture

w' lateral component of velocity perturbation (component parallel to plane of unperturbed flame front and normal to u' and v' components)

X_1, X_2 amplitude coefficients of lateral velocity component associated with pressure wave in combustible mixture

3493

x_b coordinate in x_b,y-system measured in direction of unperturbed flame-front travel relative to which burned gas is at rest

x_c coordinate in x_c,y-system measured in direction of unperturbed flame-front travel relative to which combustible mixture is at rest

$x_{1,b}$ coordinate in $x_{1,b}$,$x_{2,b}$,$x_{3,b}$-system measured in direction of unperturbed flame-front travel relative to which burned gas is at rest

$x_{2,b}$ coordinate orthogonal to $x_{1,b}$ and $x_{3,b}$ and making angle θ with y-coordinate

$x_{3,b}$ coordinate orthogonal to $x_{1,b}$ and $x_{2,b}$

$x_{1,c}$ coordinate in $x_{1,c}$,$x_{2,c}$,$x_{3,c}$-system measured in direction of unperturbed flame-front travel relative to which combustible mixture is at rest

$x_{2,c}$ coordinate orthogonal to $x_{1,c}$ and $x_{3,c}$ and making angle θ with y-coordinate

$x_{3,c}$ coordinate orthogonal to $x_{1,c}$ and $x_{2,c}$

y coordinate orthogonal to x_c and x_b

$\underline{dZ_i}(\underline{k},t)$ random amplitude vector of shear-field Fourier component

z coordinate orthogonal to x_c and y

$\alpha_1,\alpha_2 \cdot \cdot \cdot \alpha_5$ grouping defined in eqs. (B18)

Γ $\dfrac{(\gamma - 1)nr_2 T_c^{n-\frac{1}{2}}M}{\sqrt{\gamma R_g}}$

γ ratio of specific heats

Δ $\tau^2(\tau - 1)^2\tan^4\varphi + 2\tau(\tau^2 + 2\tau - 1)\tan^2\varphi + (\tau + 1)^2$

$\delta_1,\delta_2 \cdot \cdot \cdot \delta_6$ grouping defined in eqs. (B24)

$\epsilon_1, \epsilon_2 \cdots \epsilon_{10}$ grouping defined in eqs. (B21)

ζ variable upon which pressure wave depends, eqs. (7)

η variable upon which pressure wave depends, eqs. (7)

θ angle between polarization plane of incident shear wave and $x_{1,c}, x_{2,c}$-plane

Λ coefficient defined in eq. (3e)

ν $k_1' x_c + k_2' y$

$\xi'(y,t)$ flame-front displacement

ξ_t' flame-front displacement velocity

$\xi_{x_{2,c}}'$ flame-front slope with respect to $x_{2,c}$-coordinate

$\xi_{x_{3,c}}'$ flame-front slope with respect to $x_{3,c}$-coordinate

ξ_y' flame-front slope with respect to y-coordinate

ρ static density

ρ' static-density perturbation

σ $k_1' U t + k_2' y$, eq. (10j)

τ flame-temperature ratio, $T_{S,b}/T_{S,c}$

$\Phi_{ij}(\underline{k},t)$ spectral density tensor

φ angle between wave-number vector of incident shear wave and direction of unperturbed flame-front travel, $\tan \varphi \equiv k_2'/k_1'$

ψ $\left(\dfrac{U}{U-V}\right) k_1' x_b + k_2' y$

Ω scalar amplitude function defining spectral density tensor

Subscripts:

1,2,3 orthogonal coordinate designation

b   burned gas

c   combustible mixture

cr   critical

$\circledN$ designates order of steady-flow quantity

p   potential-flow velocity component

s   shear-flow velocity component

Superscripts:

$\circledN$ designates order of fluctuation quantity

*   denotes complex conjugate

'   denotes fluctuation quantity except where otherwise
                         specified

APPENDIX B

ATTENUATING-WAVE SOLUTION FOR SINGLE-WAVE INTERACTION

The arguments of the various fluctuation quantities are equal at the flame front where $x_c = Ut$ and $x_b = (U - V)t$. Therefore, substituting equations (10) into equations (3) and (5) and separately equating the real terms and the imaginary terms provide the following set of equations:

$$\left.\begin{aligned} J_1\left(1 + \frac{B_1}{\gamma}\right) + B_1L_1 - B_2N_1 - B_2G_1 &= -B_2A\sin\varphi - B_2W_1 + B_3R_1 \\ J_2\left(1 + \frac{B_1}{\gamma}\right) + B_1L_2 - B_2N_2 - B_2G_2 &= -B_2W_2 + B_3R_2 \end{aligned}\right\} \quad \text{(B1)}$$

$$\left.\begin{aligned} J_1\left(1 - \frac{1}{\gamma}\right) - L_1 - K_1N_1 - K_1G_1 &= -K_4W_1 - K_4A\sin\varphi + K_2R_1 + K_3\tau' - (K_1 - K_4)H_1 \\ J_2\left(1 - \frac{1}{\gamma}\right) - L_2 - K_1N_2 - K_1G_2 &= -K_4W_2 + K_2R_2 - (K_1 - K_4)H_2 \end{aligned}\right\}$$

$$\text{(B2)}$$

$$\left.\begin{aligned} \frac{1}{\gamma}J_1 + L_1 + (D_1 - 1)H_1 - D_1N_1 - D_1G_1 &= -W_1 - A\sin\varphi + \frac{1}{\gamma}R_1 \\ \frac{1}{\gamma}J_2 + L_2 + (D_1 - 1)H_2 - D_1N_2 - D_1G_2 &= -W_2 + \frac{1}{\gamma}R_2 \end{aligned}\right\} \quad \text{(B3)}$$

$$\left.\begin{aligned} P_1 + I_1 &= X_1 - \frac{k_1'}{k_2'}A\sin\varphi + \frac{k_2'}{k_1'}E_1H_1 \\ P_2 + I_2 &= X_2 + \frac{k_2'}{k_1'}E_1H_2 \end{aligned}\right\} \quad \text{(B4)}$$

$$\left.\begin{aligned} -f_b\left(\frac{U - V}{U}\right)N_1 - d_bN_2 &= m^2(-f_bJ_1 + b_bJ_2) \\ d_bN_1 - f_b\left(\frac{U - V}{U}\right)N_2 &= m^2(-b_bJ_1 - f_bJ_2) \end{aligned}\right\} \quad \text{(B5)}$$

$$-f_b\left(\frac{U - V}{U}\right)P_1 - d_b P_2 = m^2 c_b J_2 \left.\right\}$$
$$d_b P_1 - f_b\left(\frac{U - V}{U}\right)P_2 = - m^2 c_b J_1 \left.\right\}$$

$$(B6)$$

$$-k_1\left(\frac{U}{U - V}\right)G_2 = k_2 I_2 \left.\right\}$$
$$-k_1\left(\frac{U}{U - V}\right)G_1 = k_2 I_1 \left.\right\}$$

$$(B7)$$

$$f_c W_1 - d_c W_2 = \frac{1}{\gamma M^2}\left(f_c R_1 + b_c R_2\right) \left.\right\}$$
$$d_c W_1 + f_c W_2 = \frac{1}{\gamma M^2}\left(-b_c R_1 + f_c R_2\right) \left.\right\}$$

$$(B8)$$

$$f_c X_1 - d_c X_2 = \frac{1}{\gamma M^2} c_c R_2 \left.\right\}$$
$$d_c X_1 + f_c X_2 = - \frac{1}{\gamma M^2} c_c R_1 \left.\right\}$$

$$(B9)$$

$$H_1 - W_1 - A \sin \varphi = \Delta R_1 \left.\right\}$$
$$H_2 - W_2 = \Delta R_2 \left.\right\}$$

$$(B10)$$

From equations (B5), (B6), (B8), (B9), and (B10),

$$N_1 = h_1(h_2 J_1 - h_3 J_2) \left.\right\}$$
$$N_2 = h_1(h_3 J_1 + h_2 J_2) \left.\right\}$$

$$(B11)$$

$$P_1 = h_1(-h_4 J_1 - h_5 J_2) \left.\right\}$$
$$P_2 = h_1(h_5 J_1 - h_4 J_2) \left.\right\}$$

$$(B12)$$

$$W_1 = h_6(h_7 R_1 + h_8 R_2) \left.\right\}$$
$$W_2 = h_6(-h_8 R_1 + h_7 R_2) \left.\right\}$$

$$(B13)$$

$$X_1 = h_6(-h_9 R_1 + h_{10} R_2) \left.\right\}$$
$$X_2 = h_6(-h_{10} R_1 - h_9 R_2) \left.\right\}$$

$$(B14)$$

$$H_1 = \Delta R_1 + A \sin \varphi + h_6(h_7 R_1 + h_8 R_2)$$
$$H_2 = \Delta R_2 + h_6(-h_8 R_1 + h_7 R_2)$$
$$(B15)$$

where

$$h_1 \equiv \frac{m^2}{f_b^2/D_1^2 + d_b^2} \qquad h_6 \equiv \frac{1}{\gamma M^2(f_c^2 + d_c^2)}$$

$$h_2 \equiv \frac{f_b^2}{D_1} - b_b D_b \qquad h_7 \equiv f_c^2 - b_c d_c$$

$$h_3 \equiv \frac{b_b f_b}{D_1} + d_b f_b \qquad h_8 \equiv b_c f_c + d_c f_c$$

$$h_4 \equiv c_b d_b \qquad h_9 \equiv c_c d_c$$

$$h_5 \equiv \frac{c_b f_b}{D_1} \qquad h_{10} \equiv c_c f_c$$

$$m^2 \equiv a_b^2/\gamma U^2$$

$$(B16)$$

From equations (B4), (B7), (B12), (B14), and (B15),

$$G_1 = \alpha_1 R_1 - \alpha_2 R_2 - \alpha_3 J_1 - \alpha_4 J_2 + \alpha_5 A \sin \varphi$$
$$G_2 = \alpha_2 R_1 + \alpha_1 R_2 + \alpha_4 J_1 - \alpha_3 J_2$$
$$(B17)$$

where

$$\alpha_1 \equiv \frac{k_2'}{k_1' D_1} \left[\frac{-k_2' E_1}{k_1'} (\Delta + h_6 h_7) + h_6 h_9 \right]$$

$$\alpha_2 \equiv \frac{k_2'}{k_1' D_1} \left[\frac{k_2' E_1}{k_1'} h_6 h_8 + h_6 h_{10} \right]$$

$$\alpha_3 \equiv \frac{k_2'}{k_1' D_1} h_1 h_4$$

$$\alpha_4 \equiv \frac{k_2'}{k_1' D_1} h_1 h_5$$

$$\alpha_5 \equiv \frac{1}{D_1} \left(1 - \frac{k_2'^2}{k_1'^2} E_1 \right)$$

$$(B18)$$

Then, from equation (B2),

$$
\begin{aligned}
L_1 = {}& J_1\left[1 - \frac{1}{\gamma} - K_1(h_1h_2 - \alpha_3)\right] + J_2\left[K_1(h_1h_3 + \alpha_4)\right] + \\
& R_1\left[K_1(h_6h_7 - \alpha_1) - K_2 + (K_1 - K_4)\Lambda\right] + \\
& R_2\left[K_1(h_6h_8 + \alpha_2)\right] + A \sin \varphi\left[K_1(1 - \alpha_5)\right] - K_3\tau' \\
L_2 = {}& - J_1\left[K_1(h_1h_3 + \alpha_4)\right] + J_2\left[1 - \frac{1}{\gamma} - K_1(h_1h_2 - \alpha_3)\right] - R_1\left[K_1(h_6h_8 + \alpha_2)\right] + \\
& R_2\left[K_1(h_6h_7 - \alpha_1) - K_2 + (K_1 - K_4)\Lambda\right]
\end{aligned}
\tag{B19}
$$

The various disturbance amplitude coefficients of equations (10) have now been obtained in terms of the coefficients R_1, R_2, J_1, J_2 and the parameters $A \sin \varphi$ and τ'. From equations (B1) and (B3),

$$
\left.
\begin{aligned}
J_1\varepsilon_1 + J_2\varepsilon_2 + R_1\varepsilon_3 + R_2\varepsilon_4 &= \varepsilon_5 \\
-J_1\varepsilon_2 + J_2\varepsilon_1 - R_1\varepsilon_4 + R_2\varepsilon_3 &= 0 \\
J_1\varepsilon_6 + J_2\varepsilon_7 + R_1\varepsilon_8 + R_2\varepsilon_9 &= \varepsilon_{10} \\
-J_1\varepsilon_7 + J_2\varepsilon_6 - R_1\varepsilon_9 + R_2\varepsilon_8 &= 0
\end{aligned}
\right\}
\tag{B20}
$$

where

$$
\left.
\begin{aligned}
\varepsilon_1 &\equiv 1 + B_1 - (B_1K_1 + B_2)(h_1h_2 - \alpha_3) \\
\varepsilon_2 &\equiv (B_1K_1 + B_2)(h_1h_3 + \alpha_4) \\
\varepsilon_3 &\equiv (B_1K_1 + B_2)(h_6h_7 - \alpha_1) + B_1(K_1 - K_4)\Lambda - B_3 - B_1K_2 \\
\varepsilon_4 &\equiv (B_1K_1 + B_2)(h_6h_8 + \alpha_2) \\
\varepsilon_5 &\equiv B_1K_3\tau' - A \sin \varphi\left[(B_1K_1 + B_2)(1 - \alpha_5)\right] \\
\varepsilon_6 &\equiv 1 - (D_1 + K_1)(h_1h_2 - \alpha_3) \\
\varepsilon_7 &\equiv (D_1 + K_1)(h_1h_3 + \alpha_4) \\
\varepsilon_8 &\equiv (D_1 + K_1)(h_6h_7 - \alpha_1) + (D_1 - 1)\Lambda - \left(K_2 + \frac{1}{\gamma}\right) + (K_1 - K_4)\Lambda \\
\varepsilon_9 &\equiv (D_1 + K_1)(h_6h_8 + \alpha_2) \\
\varepsilon_{10} &\equiv K_3\tau' - A \sin \varphi(D_1 + K_1)(1 - \alpha_5)
\end{aligned}
\right\}
\tag{B21}
$$

or

$$J_1 = \frac{R_1(\epsilon_1\epsilon_9 - \epsilon_4\epsilon_6) - R_2(\epsilon_1\epsilon_8 - \epsilon_3\epsilon_6)}{\epsilon_2\epsilon_6 - \epsilon_1\epsilon_7}$$

$$J_2 = \frac{R_1(\epsilon_2\epsilon_9 - \epsilon_4\epsilon_7) - R_2(\epsilon_2\epsilon_8 - \epsilon_3\epsilon_7)}{\epsilon_2\epsilon_6 - \epsilon_1\epsilon_7}$$

$$\left.\right\}$$ (B22)

$$R_1 = \frac{\delta_2\delta_6 - \delta_3\delta_5}{\delta_2\delta_4 - \delta_1\delta_5}$$

$$R_2 = \frac{\delta_1\delta_6 - \delta_3\delta_4}{\delta_2\delta_4 - \delta_1\delta_5}$$

$$\left.\right\}$$ (B23)

where

$$\delta_1 \equiv \epsilon_1(\epsilon_1\epsilon_9 - \epsilon_4\epsilon_6) + \epsilon_3(\epsilon_2\epsilon_6 - \epsilon_1\epsilon_7) - \epsilon_2(\epsilon_4\epsilon_7 - \epsilon_2\epsilon_9)$$

$$\delta_2 \equiv \epsilon_1(\epsilon_1\epsilon_8 - \epsilon_3\epsilon_6) - \epsilon_4(\epsilon_2\epsilon_6 - \epsilon_1\epsilon_7) - \epsilon_2(\epsilon_3\epsilon_7 - \epsilon_2\epsilon_8)$$

$$\delta_3 \equiv \epsilon_5(\epsilon_2\epsilon_6 - \epsilon_1\epsilon_7)$$

$$\delta_4 \equiv \epsilon_6(\epsilon_1\epsilon_9 - \epsilon_4\epsilon_6) + \epsilon_8(\epsilon_2\epsilon_6 - \epsilon_1\epsilon_7) - \epsilon_7(\epsilon_4\epsilon_7 - \epsilon_2\epsilon_9)$$

$$\delta_5 \equiv \epsilon_6(\epsilon_1\epsilon_8 - \epsilon_3\epsilon_6) - \epsilon_7(\epsilon_3\epsilon_7 - \epsilon_2\epsilon_8) - \epsilon_9(\epsilon_2\epsilon_6 - \epsilon_1\epsilon_7)$$

$$\delta_6 \equiv \epsilon_{10}(\epsilon_2\epsilon_6 - \epsilon_1\epsilon_7)$$

$$\left.\right\}$$ (B24)

Equations (B11) to (B15), (B17), (B19), (B22), and (B23) provide the formal solution of equations (B1) to (B10).

APPENDIX C

ATTENUATING-WAVE SOLUTION FOR CONSTANT-PRESSURE COMBUSTION

If terms of order M^2 are retained, equations (1) provide the following relations for the unperturbed flow quantities:

$$\frac{p_b}{p_c} = 1 - \gamma(\tau - 1)M^2 + \ldots$$

$$\frac{\rho_c}{\rho_b} = \frac{U - V}{U} = \tau\left[1 + \frac{\gamma + 1}{2}(\tau - 1)M^2 + \ldots\right]$$

$$\frac{c_p T_{S,c}}{U^2} = \frac{1}{2} + \frac{1}{(\gamma - 1)M^2}$$

$$\frac{U^2}{a_b^2} = \frac{2M^2}{\tau\left[2 - (\gamma - 1)(\tau - 1)M^2 - (\gamma^2 - 1)\tau(\tau - 1)M^4 + \ldots\right]}$$

With these relations, equations (4) take the form

$$\left.\begin{aligned}
&B_1 = \gamma\tau M^2, \quad B_2 = 2\gamma M^2, \quad B_3 = 1 + \left[1 + \gamma(\tau - 1)\right]M^2 \\[2mm]
&D_1 = \frac{1}{\tau}\left[1 - \frac{\gamma + 1}{2}(\tau - 1)M^2\right], \quad E_1 = (\tau - 1)\left[1 + \frac{\gamma + 1}{2}\tau M^2\right] \\[2mm]
&K_1 = K_4 = (\gamma - 1)M^2, \quad K_2 = \frac{\gamma - 1}{\gamma}\left[1 + \frac{\gamma - 1}{2}(\tau - 1)M^2\right], \quad K_3 = \frac{1}{\tau} + \frac{\gamma - 1}{2}M^2
\end{aligned}\right\}$$

$$\text{(C1)}$$

and equations (9) may be written

$$\left.\begin{aligned}
&b_c = b_b = -k_1' M^2, \quad c_c = c_b = k_2', \quad d_c = k_1'(1 + M^2), \quad d_b = k_1'(1 + \tau M^2) \\[2mm]
&f_c^2 = k_2'^2 - (k_1'^2 - k_2'^2)M^2, \quad f_b^2 = k_2'^2 - \left(\frac{k_1'^2 - \tau^2 k_2'^2}{\tau}\right)M^2
\end{aligned}\right\}$$

$$\text{(C2)}$$

If only the leading terms in powers of M^2 are retained, equations (B16) and (B18) of appendix B provide the following relations:

$$\left.\begin{aligned}
h_1h_2 = h_1h_5 &= \frac{\tau^2\tan^2\varphi}{\gamma M^2(1 + \tau^2\tan^2\varphi)}, & h_1h_3 = h_1h_4 &= \frac{\tau\,\tan\,\varphi}{\gamma M^2(1 + \tau^2\tan^2\varphi)}\\
h_6h_7 = h_6h_{10} &= \frac{\sin^2\varphi}{\gamma M^2}, & h_6h_8 = h_6h_9 &= \frac{\sin\,\varphi\,\cos\,\varphi}{\gamma M^2}
\end{aligned}\right\} \quad (C3)$$

and

$$\left.\begin{aligned}
\alpha_1 &= \frac{\tau\,\sin^2\varphi}{\gamma M^2}\left[1 - (\tau - 1)\tan^2\varphi\right]\\
\alpha_2 &= \frac{\tau^2\sin^2\varphi\,\tan\,\varphi}{\gamma M^2}\\
\alpha_3 &= \frac{\tau^2\tan^2\varphi}{\gamma M^2(1 + \tau^2\tan^2\varphi)}\\
\alpha_4 &= \frac{\tau^3\tan^3\varphi}{\gamma M^2(1 + \tau^2\tan^2\varphi)}\\
\alpha_5 &= \tau\left[1 - (\tau - 1)\tan^2\varphi\right]
\end{aligned}\right\} \quad (C4)$$

From these relations:

$$\left.\begin{aligned}
h_1h_3 + \alpha_4 &= \frac{\tau\,\tan\,\varphi}{\gamma M^2}, & h_6h_7 - \alpha_1 &= \frac{(\tau - 1)\sin^2\varphi(\tau\,\tan^2\varphi - 1)}{\gamma M^2}\\
h_1h_2 - \alpha_3 &= 0, & h_6h_8 + \alpha_2 &= \frac{\sin\,\varphi\,\cos\,\varphi(1 + \tau^2\tan^2\varphi)}{\gamma M^2}
\end{aligned}\right\} \quad (C5)$$

From equations (B21) and (C5),

$$\left.\begin{aligned}
\varepsilon_1\varepsilon_9 - \varepsilon_4\varepsilon_6 &= \frac{\sin\,\varphi\,\cos\,\varphi(1 + \tau^2\tan^2\varphi)}{\gamma M^2\tau}\\
\varepsilon_1\varepsilon_8 - \varepsilon_3\varepsilon_6 &= \frac{(\tau - 1)\sin^2\varphi(\tau\,\tan^2\varphi - 1)}{\gamma M^2\tau}\\
\varepsilon_3\varepsilon_7 - \varepsilon_2\varepsilon_8 = \varepsilon_2\varepsilon_6 - \varepsilon_1\varepsilon_7 &= -\frac{\tan\,\varphi}{\gamma M^2}, \quad \varepsilon_4\varepsilon_7 - \varepsilon_2\varepsilon_9 = 0
\end{aligned}\right\} \quad (C6)$$

and from equations (B21), (B24), and (C6):

$$\delta_1 = \frac{\sin \varphi \cos \varphi}{\gamma M^2 \tau}\left[(\tau + 1)(1 + \tau \tan^2\varphi) - 2 \tan^2\varphi(\tau - 1)\tau(\tau \tan^2\varphi - 1)\right]$$

$$\delta_2 = \frac{\sin^2\varphi}{\gamma M^2 \tau}\left[(\tau - 1)(\tau \tan^2\varphi - 1) + 2(\tau + 1)\tau(\tau \tan^2\varphi + 1)\right]$$

$$\delta_3 = - \tan \varphi\left[\tau' - 2(\tau - 1)(\tau \tan^2\varphi - 1)A \sin \varphi\right]$$

$$\delta_4 = \frac{-(\tau - 1)\tan \varphi \sin^2\varphi(\tau \tan^2\varphi - 1)}{\gamma^2 M^4 \tau}$$

$$\delta_5 = \frac{(\tau + 1)(\tau \tan^2\varphi + 1)\sin^2\varphi}{\gamma^2 M^4 \tau}$$

$$\delta_6 = - \frac{\tan \varphi}{\gamma M^2 \tau}\left[\tau' - (\tau - 1)(\tau \tan^2\varphi - 1)A \sin \varphi\right]$$

$$(C7)$$

Since for constant-pressure combustion $R^{(1)} \equiv R_2/\gamma M^2$, $R^{(2)} \equiv R_2/\gamma M^2$, and so forth, the coefficients $R^{(1)}$, $R^{(2)}$, $J^{(1)}$, and $J^{(2)}$ are obtained from equations (B22), (B23), (C6), and (C7). With these coefficients determined, the remainder are obtained from equations (B7), (B11) to (B14), (B17), and (B19). The amplitude coefficients are

$$R^{(1)} = \frac{-1}{\Delta}\left\{(\tau-1)^2(\tau\,\tan^2\varphi - 1)^2 A\,\sin\varphi - \left[\tau^2(\tau^2 + 2\tau - 1)\tan^2\varphi + \tau(\tau^2+1)\right]\frac{\tau'}{\tau}\right\}$$

$$R^{(2)} = J^{(2)} = -\frac{1}{\Delta\,\tan\varphi}\left\{(\tau^2-1)(\tau^2\tan^4\varphi - 1)A\,\sin\varphi + \left[\tau^3(\tau-1)\tan^4\varphi - 2\tau^3\tan^2\varphi - \tau(\tau+1)\right]\frac{\tau'}{\tau}\right\}$$

$$J^{(1)} = -\frac{1}{\Delta}\left\{(\tau-1)^2(\tau\,\tan^2\varphi - 1)^2 A\,\sin\varphi + \tau^2\left[\tau(\tau-1)^2\tan^4\varphi + (\tau^2+2\tau-1)\tan^2\varphi + 2\right]\frac{\tau'}{\tau}\right\}$$

$$L_1 = -\frac{\tau'}{\tau}, \quad L_2 = 0$$

$$N_1 = \frac{\tau}{\Delta(1+\tau^2\tan^2\varphi)}\left((\tau-1)(\tau\,\tan^2\varphi - 1)\left[(\tau+1)(\tau\,\tan^2\varphi + 1) - \tau(\tau-1)\tan^2\varphi(\tau\,\tan^2\varphi - 1)\right]A\,\sin\varphi - \right.$$
$$\left. \tau\left\{\tau^2\tan^2\varphi\left[\tau(\tau-1)^2\tan^4\varphi + \tau(\tau+1)\tan^2\varphi + 4\right] + (\tau+1)\right\}\frac{\tau'}{\tau}\right)$$

$$N_2 = \frac{-\tau(\tau-1)\tan\varphi}{\Delta(1+\tau^2\tan^2\varphi)}\left\{(\tau\,\tan^2\varphi - 1)\left[\tau(\tau+1)(\tau\,\tan^2\varphi + 1) + (\tau-1)(\tau\,\tan^2\varphi - 1)\right]A\,\sin\varphi + \right.$$
$$\left. \tau^2\left[\tau(2\tau-1)\tan^4\varphi - (\tau-1)\tan^2\varphi - 1\right]\frac{\tau'}{\tau}\right\}$$

$$G_1 = \frac{\tau}{\Delta(1+\tau^2\tan^2\varphi)}\left\{\left[(\tau+1)^2(\tau\,\tan^2\varphi + 1)^2 + \tau(\tau-1)^2\tan^2\varphi(\tau\,\tan^2\varphi - 1)^2\right]A\,\sin\varphi - \right.$$
$$\left. \tau(\tau-1)\tan^2\varphi\left[\tau(\tau^2+2\tau-1)\tan^2\varphi + (\tau^2+1)\right]\frac{\tau'}{\tau}\right\}$$

$$G_2 = \frac{(\tau-1)\tan\varphi}{\Delta(1+\tau^2\tan^2\varphi)}\left\{(\tau^2-1)(\tau\,\tan^2\varphi - 1)(\tau\,\tan^2\varphi + 1)A\,\sin\varphi + \left[\tau^3(\tau-1)\tan^4\varphi - 2\tau^3\tan^2\varphi - \tau(\tau+1)\right]\frac{\tau'}{\tau}\right\}$$

$$P_1 = -N_2, \quad P_2 = N_1$$

$$I_1 = \frac{G_1}{\tau\,\tan\varphi}, \quad I_2 = \frac{-G_2}{\tau\,\tan\varphi}$$

$$W_1 = -\frac{1}{\Delta}\left\{(\tau-1)(\tau\,\tan^2\varphi - 1)\left[\tau(\tau-1)\tan^2\varphi + (\tau+1)\right]A\,\sin\varphi - \left[\tau^2(3\tau-1)\tan^2\varphi + \tau(\tau+1)\right]\frac{\tau'}{\tau}\right\}$$

$$W_2 = -\frac{\tau(\tau-1)\tan\varphi}{\Delta}\left\{2(\tau\,\tan^2\varphi - 1)A\,\sin\varphi + \tau\left[\tau\,\tan^2\varphi + 1\right]\frac{\tau'}{\tau}\right\}$$

$$X_1 = H_2 = W_2, \quad X_2 = -W_1$$

$$H_1 = \frac{\tau}{\Delta}\left\{2(\tau+1)(\tau\,\tan^2\varphi + 1)A\,\sin\varphi + \left[\tau(3\tau-1)\tan^2\varphi + (\tau+1)\right]\frac{\tau'}{\tau}\right\}$$

$$\left.\right\} \quad (C8)$$

For constant-pressure combustion $\zeta_c = \zeta_b = k_1' Ut + k_2' y$,

$\eta_c = k_2' (x_c - Ut)$, $\eta_b = k_2'[-x_b + (U - V)t]$, $\nu = k_1' x_c + k_2' y$,

$\psi = \dfrac{k_1' x_b}{\tau} + k_2' y$, and $\sigma = k_1' Ut + k_2' y$. At the flame front where $x_c = Ut$

and $x_b = (U - V)t$, $\eta_c = \eta_b = 0$, the attenuation factors $e^{-\eta_c}$ and $e^{-\eta_b}$
are unity, and the arguments of the disturbance waves have the form
$(k_1' Ut + k_2' y)$.

The procedure of reference 23 is utilized in reference 22 to treat
a similar interaction problem for consideration of flame-front stability.
It is assumed that there are first-order perturbations in the laminar
flame speed U (in the present notation). Reference 22 presents results
only for the special case where the plane of polarization of the inci-
dent shear wave is in the plane $x_{1,c} - x_{2,c} (\theta = 0^\circ)$ and the wave-number
vector is parallel to the unperturbed flame front ($\varphi = 90^\circ$). The re-
sults of the present analysis were compared with those of reference 22
for the case of an absence of first-order perturbations in the laminar
flame speed and for the special case of $\theta = 0^\circ$ and $\varphi = 90^\circ$ without
heat-release perturbations. Although agreement as to sign and magnitude
is obtained for the shear-field velocity components, apparently differ-
ences in sign occur for the potential-field velocity-component ampli-
tudes as indicated in the following table:

	Present analysis	Analysis of reference 22
$\dfrac{u_{p,c}'}{U}$	-A	-A
$\dfrac{v_{p,c}'}{U}$	iA	-iA
$\dfrac{u_{p,b}'}{U}$	A	-A
$\dfrac{v_{p,b}'}{U}$	iA.	iA

Consideration of conservation of momentum across the flame front indi-
cates that $v_{p,c}'/U$ and $v_{p,b}'/U$ should be of the same sign. The pres-
ent analysis is in agreement with this consideration.

REFERENCES

1. Damkohler, Gerhard: The Effect of Turbulence on the Flame Velocity in Gas Mixtures. NACA TM 1112, 1947.

2. Shelkin, K. I.: On Combustion in a Turbulent Flow. NACA TM 1110, 1947.

3. Bollinger, Lowell M., and Williams, David T.: Effect of Reynolds Number in the Turbulent-Flow Range on Flame Speeds of Bunsen Burner Flames. NACA Rep. 932, 1949. (Supersedes NACA TN 1707.)

4. Williams, G. C., Hottel, H. C., and Scurlock, A. C.: Flame Stabilization and Propagation in High Velocity Gas Streams. Third Symposium on Combustion and Flame and Explosion Phenomena, The Williams & Wilkins Co. (Baltimore), 1949, pp. 21-40.

5. Markstein, G. H.: Interaction of Flame Propagation and Flow Disturbances. Third Symposium on Combustion and Flame and Explosion Phenomena, The Williams & Wilkins Co. (Baltimore), 1949, pp. 162-167.

6. Karlovitz, Béla, Denniston, D. W., Jr., and Wells, F. E.: Investigation of Turbulent Flames. Jour. Chem. Phys., vol. 19, no. 5, May 1951, pp. 541-547.

7. Scurlock, A. C., and Grover, J. H.: Propagation of Turbulent Flames. Fourth Symposium (International) on Combustion, The Williams & Wilkins Co. (Baltimore), 1953, pp. 645-658.

8. Westenberg, Arthur A.: Flame Turbulence Measurements by the Method of Helium Diffusion. Jour. Chem. Phys., vol. 22, no. 5, May 1954, pp. 814-823.

9. Wohl, K., Shore, L., Von Rosenberg, H., and Weil, C. W.: The Burning Velocity of Turbulent Flames. Fourth Symposium (International) on Combustion, The Williams & Wilkins Co. (Baltimore), 1953, pp. 620-635.

10. Batchelor, G. K.: The Theory of Homogeneous Turbulence. Cambridge Univ. Press, 1953.

11. Carrier, G. F., and Carlson, F. D.: On the Propagation of Small Disturbances in a Moving Compressible Fluid. Quarterly Appl. Math., vol. 4, no. 1, Apr. 1946, pp. 1-12.

12. Moore, Franklin K.: Unsteady Oblique Interaction of a Shock Wave
    with a Plane Disturbance. NACA Rep. 1165, 1954. (Supersedes
    NACA TN 2879.)

13. Clark, Thomas P., and Bittker, David A.: A Study of the Radiation
    from Laminar and Turbulent Open Propane-Air Flames as a Function
    of Flame Area, Equivalence Ratio, and Fuel Flow Rate. NACA RM
    E54F29, 1954.

14. Dugger, Gordon L.: Effects of Initial Mixture Temperature on Flame
    Speed of Methane-Air, Propane-Air, and Ethylene-Air Mixtures. NACA
    Rep. 1061, 1952. (Supersedes NACA TN's 2170 and 2374.)

15. Moyal, J. E.: The Spectra of Turbulence in a Compressible Fluid;
    Eddy Turbulence and Random Noise. Proc. Cambridge Phil. Soc.,
    vol. 48, pt. 2, Apr. 1952, pp. 329-344.

16. Ribner, H. S.: Shock-Turbulence Interaction and the Generation of
    Noise. NACA TN 3255, 1954.

17. Ribner, H. S., and Tucker, M.: Spectrum of Turbulence in a Con-
    tracting Stream. NACA Rep. 1113, 1953. (Supersedes NACA TN 2606.)

18. Morse, Philip M.: Vibration and Sound. Second ed., McGraw-Hill
    Book Co., Inc., 1948.

19. Hottel, H. C., Williams, G. C., and Satterfield, C. N.: Thermody-
    namic Charts for Combustion Processes, Pt. I. John Wiley & Sons,
    Inc., 1949.

20. Gerstein, Melvin, Levine, Oscar, and Wong, Edgar L.: Fundamental
    Flame Velocities of Pure Hydrocarbons. I - Alkanes, Alkenes,
    Alkynes, Benzene and Cyclohexane. NACA RM E50G24, 1950.

21. Levine, Oscar, and Gerstein, Melvin: Fundamental Flame Velocities
    of Pure Hydrocarbons. III - Extension of Tube Method to High Flame
    Velocities - Acetylene-Air Mixtures. NACA RM E51J05, 1951.

22. Markstein, George H.: Interaction of a Plane Flame Front with a
    Plane Sinusoidal Shear Wave. Jour. Aero. Sci., vol. 20, no. 8,
    Aug. 1953, pp. 581-582.

23. Ribner, H. S.: Convection of a Pattern of Vorticity Through a
   Shock Wave. NACA Rep. 1164, 1954. (Supersedes NACA TN 2864.)

3493

CJ-7

TABLE I. - FLAME-TURBULENCE-INTERACTION FLUCTUATION RATIOS

| τ	$\sqrt{\dfrac{\overline{\left(\frac{u_{1,s,b}}{U}\right)^2}}{\overline{\left(\frac{u_{1,s,c}}{U}\right)^2}}}$ (eq. (23c))	$\sqrt{\dfrac{\overline{\left(\frac{u_{2,s,b}}{U}\right)^2}+\overline{\left(\frac{u_{3,s,b}}{U}\right)^2}}{\overline{\left(\frac{u_{2,s,c}}{U}\right)^2}+\overline{\left(\frac{u_{3,s,c}}{U}\right)^2}}}$ (eq. (23d))	$\sqrt{\dfrac{\overline{\left(\frac{u_{1,p,b}}{U}\right)^2}}{\overline{\left(\frac{u_{1,s,c}}{U}\right)^2}}}$ (eq. (23e))	$\sqrt{\dfrac{\overline{\left(\frac{u_{1,p,c}}{U}\right)^2}}{\overline{\left(\frac{u_{1,s,c}}{U}\right)^2}}}$ (eq. (23b))	$\sqrt{\dfrac{\overline{\left(\frac{p'_c}{\rho_c U^2}\right)^2}}{\overline{\left(\frac{u_{1,s,c}}{U}\right)^2}}}$ (eq. (23a))	$\sqrt{\dfrac{\overline{(\xi_t)^2}}{\overline{\left(\frac{u_{1,s,c}}{U}\right)^2}}}$ (eq. (23f))	$\dfrac{\overline{\xi^2_{x_{2,c}}}+\overline{\xi^2_{x_{3,c}}}}{\overline{\left(\frac{u_{1,s,c}}{U}\right)^2}}$ (eq. (23g))	$\dfrac{-\overline{\frac{u_{2,c}}{U}\,\xi_{x_{2,c}}}-\overline{\frac{u_{3,c}}{U}\,\xi_{x_{3,c}}}}{\overline{\left(\frac{u_{1,s,c}}{U}\right)^2}}$ (eq. (26))
1	1.0000	1.0000	0	0	0	1.0000	∞	1.0000
1.5	.8868	.9380	------	------	------	------	6.0062	1.9553
2	.8814	.9120	.7024	.6833	.7146	.6109	2.2942	1.4270
2.25	------	------	------	------	------	------	1.6501	1.2626
3	.9103	.8904	.8235	.7823	.8358	.4686	.7974	.9439
3.5	------	------	------	------	------	------	.5559	.8098
5	.9676	.8772	.9325	.8604	.9416	.3307	.2521	.5697
7	1.0067	.8727	.9876	.8956	.9943	.2599	.1236	.4094
10	1.0452	.8700	1.0552	.9234	1.0397	.1995	.0592	.2884
15	1.0833	.8682	1.0786	.9463	1.0813	.1462	.0260	.1936
∞	1.2247	.8660	1.2247	1.0000	1.2247	0	0	0

TABLE II. - HYDROCARBON-AIR FLAME DATA AT SPECIFIED CONDITIONS

$(p_c = 760$ mm Hg; $T_c = 25^\circ$ C$)$

	Propane, C_3H_8		Ethylene, C_2H_4		Acetylene, C_2H_2	
	At stoichiometric	At maximum U	At stoichiometric	At maximum U	At stoichiometric	At maximum U
Fuel-air ratio	0.0638	0.0721	0.0676	0.0757	0.0753	0.1040
Volume percentage of fuel in air	4.04	4.54	6.54	7.65	7.75	10.70
Laminar flame speed, U, cm/sec	37.5	39	64	68	123.5	141
Adiabatic flame-temperature ratio, τ	7.70	7.45	7.95	8.00	8.64	8.71
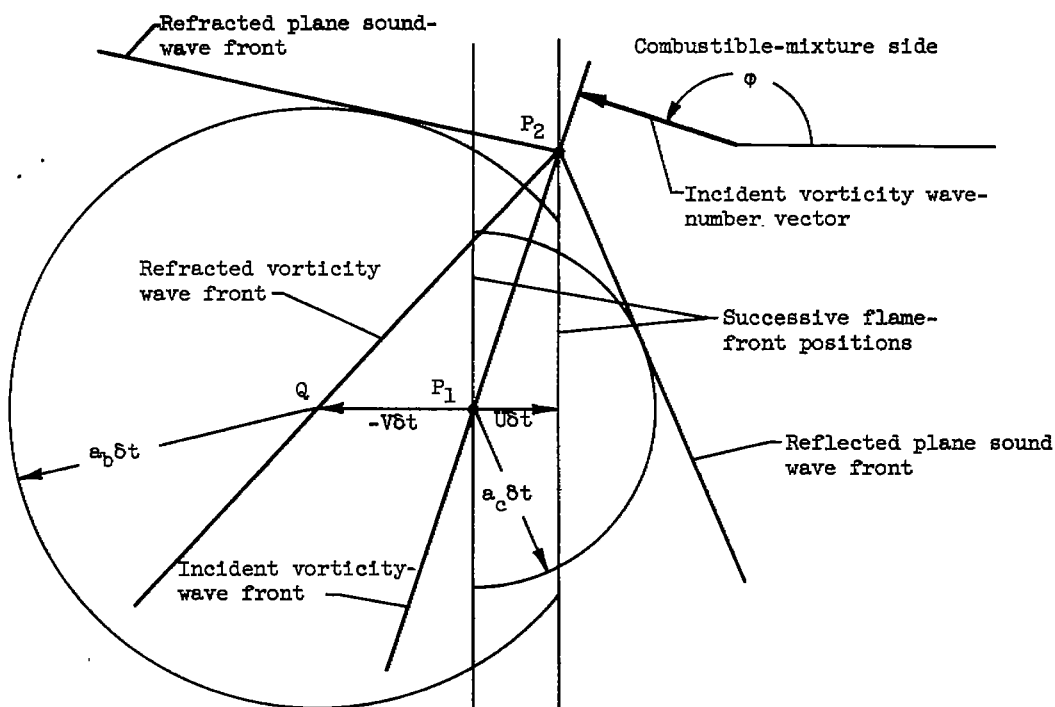
(a) Interaction for wave-number vector inclinations generating plane sound waves.
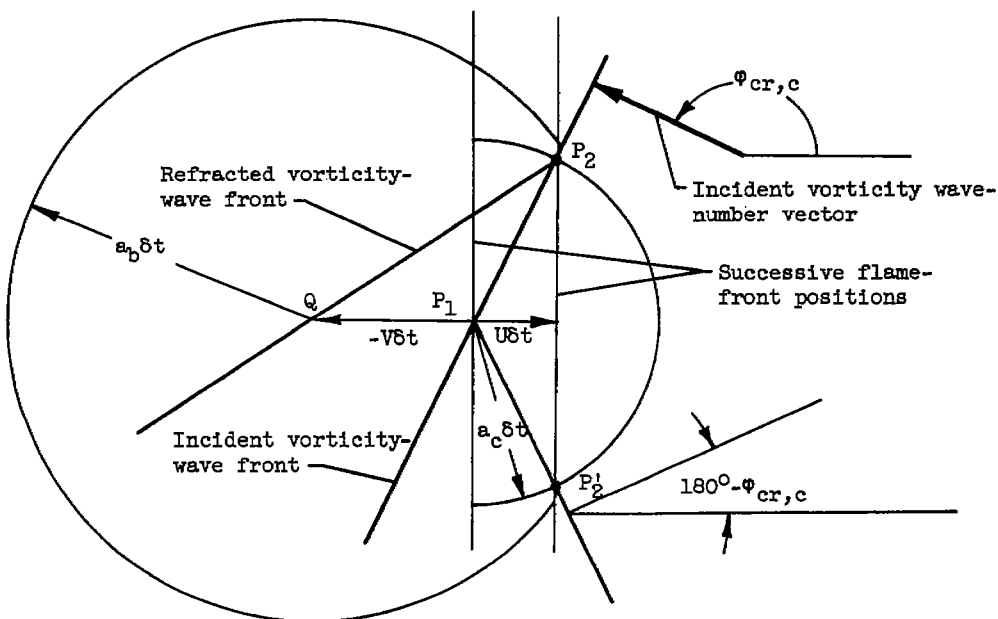
(b) Interaction for wave-number vector inclinations generating noncoalescing cylindrical sound waves.

Figure 1. - Wave formation arising from interaction of flame front with vorticity wave.

3493

The figure legend shows:

$$\sqrt{\frac{\overline{\left(\frac{u_{1,s,b}}{U}\right)^2}}{\overline{\left(\frac{u_{1,s,c}}{U}\right)^2}}} \quad (eq. \ (23c))$$

$$\sqrt{\frac{\overline{\left(\frac{u_{2,s,b}}{U}\right)^2} + \overline{\left(\frac{u_{3,s,b}}{U}\right)^2}}{\overline{\left(\frac{u_{2,s,c}}{U}\right)^2} + \overline{\left(\frac{u_{3,s,c}}{U}\right)^2}}} \quad (eq. \ (23d))$$

⎫ Shear-flow velocities ⎬

$$\sqrt{\frac{\overline{\left(\frac{u_{1,p,b}}{U}\right)^2}}{\overline{\left(\frac{u_{1,s,c}}{U}\right)^2}}} \quad (eq. \ (23e))$$

$$\sqrt{\frac{\overline{\left(\frac{u_{1,p,c}}{U}\right)^2}}{\overline{\left(\frac{u_{1,s,c}}{U}\right)^2}}} \quad (eq. \ (23b))$$
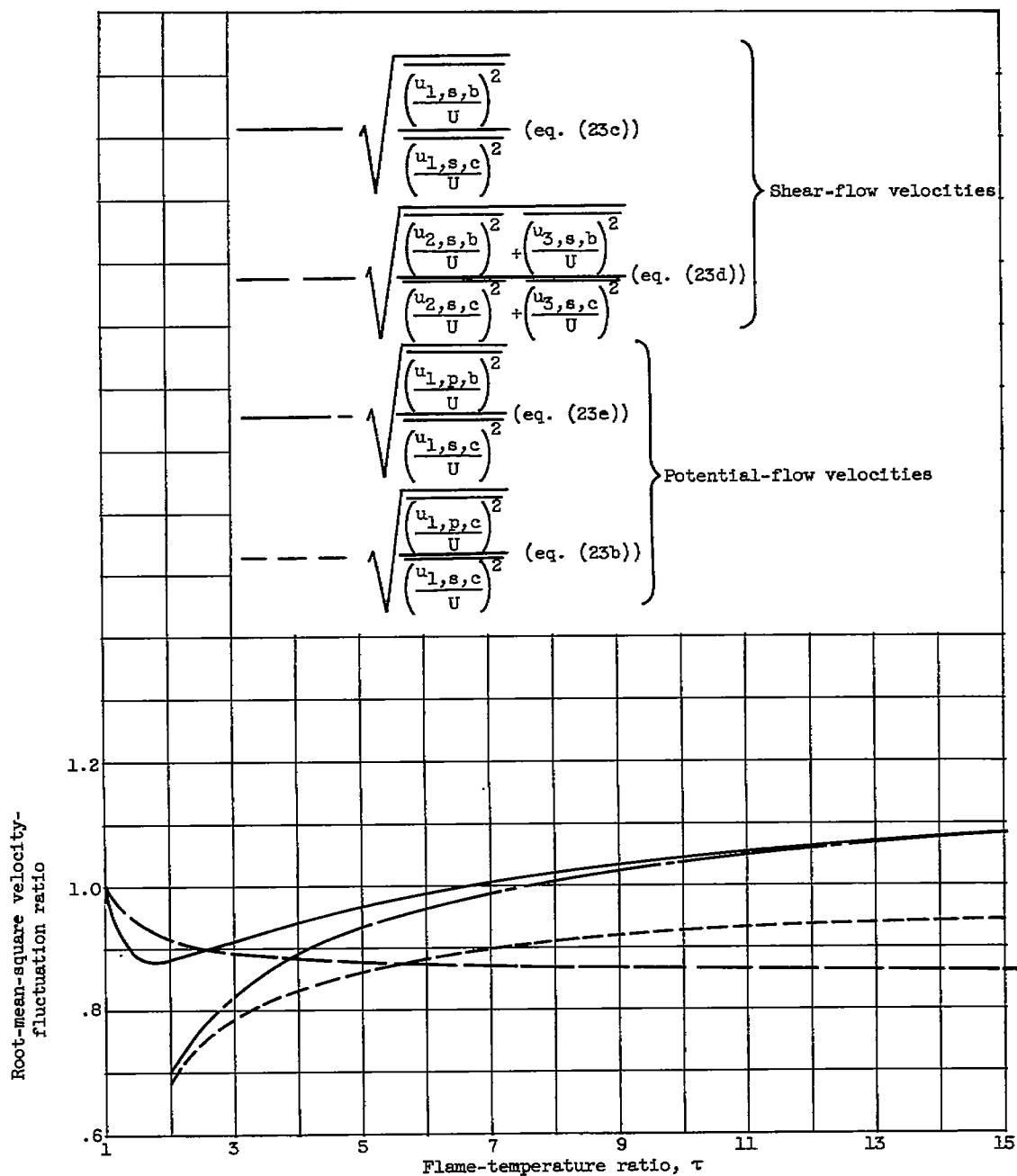
⎫ Potential-flow velocities ⎬

Figure 2. - Effect of flame-temperature ratio on shear-flow and potential-flow velocity fluctuations.
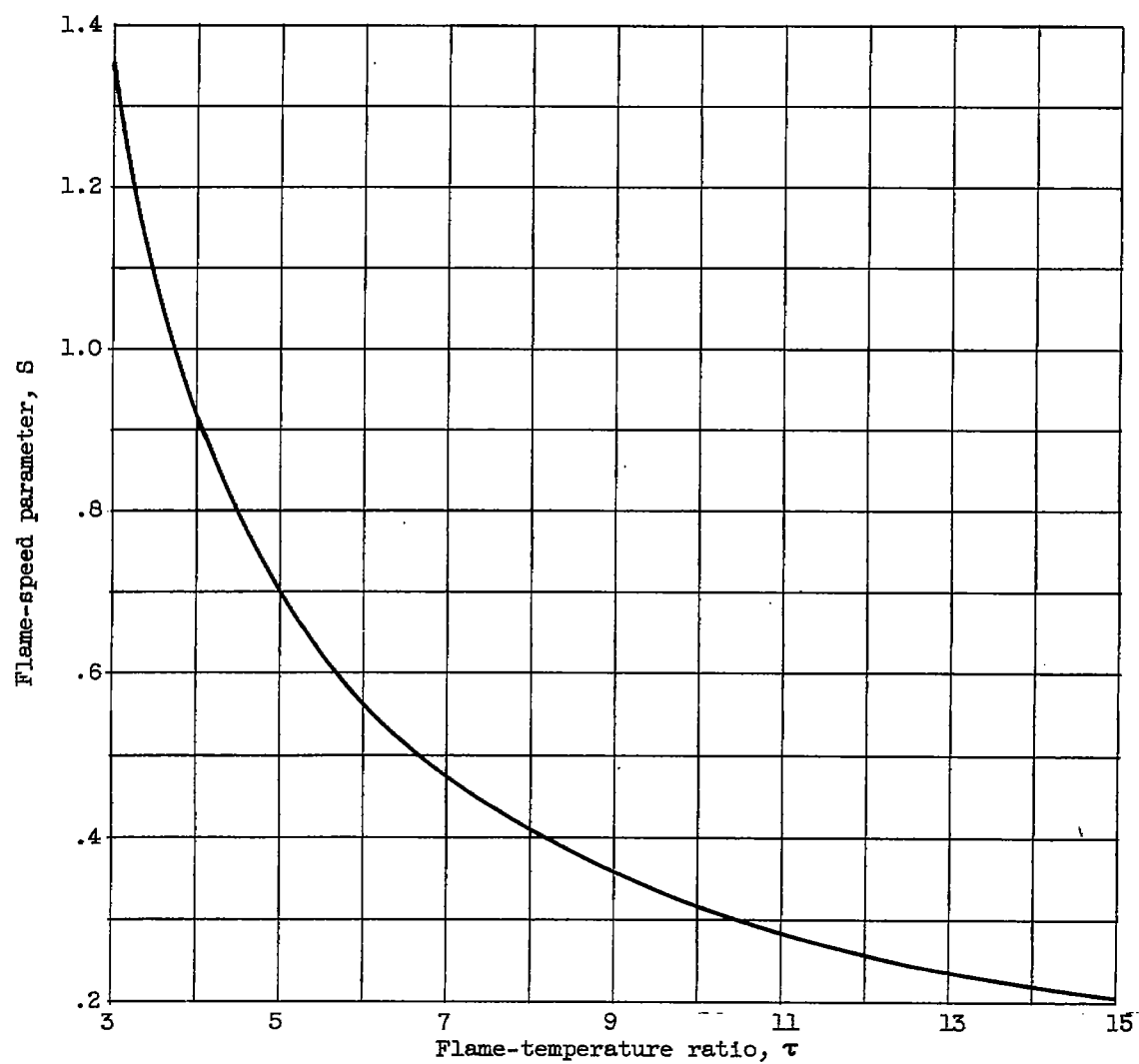
Figure 3. - Effect of flame-temperature ratio on flame speed for incident
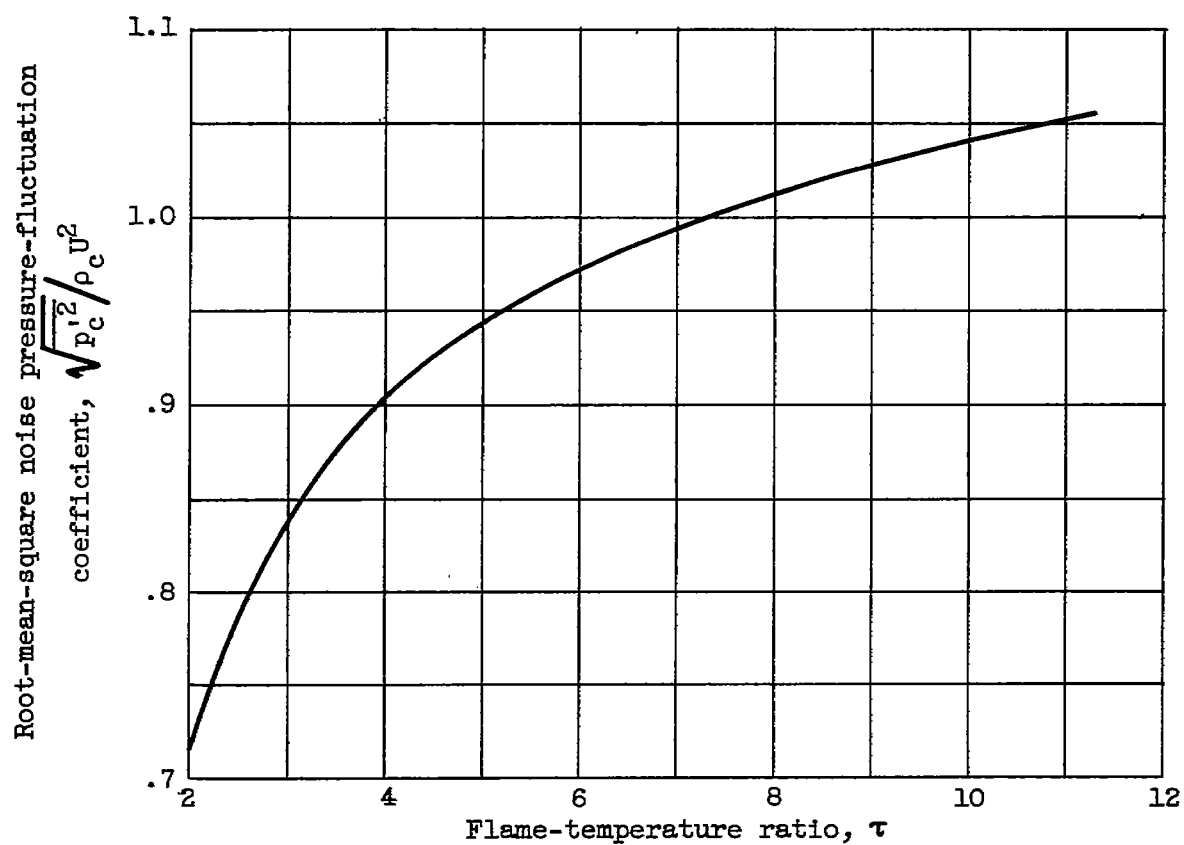isotropic turbulence.

3493

Figure 4. - Effect of flame-temperature ratio on random
pressure fluctuations generated at flame front.